Utah State University

DigitalCommons@USU

5-1964

Effects of Temperature on Moisture Conductivity in Unsaturated Soil

Richard O'Bannon Meeuwig
Utah State University

UtahState University
MERRILL-CAZIER LIBRARY

EFFECTS OF TEMPERATURE ON MOISTURE CONDUCTIVITY

IN UNSATURATED SOIL

by

Richard O'Bannon Meeuwig

A dissertation submitted in partial fulfillment
of the requirements for the degree

of

DOCTOR OF PHILOSOPHY

in

Soil Physics

UTAH STATE UNIVERSITY
Logan, Utah

1964

ACKNOWLEDGEMENTS

TABLE OF CONTENTS

LIST OF TABLES

List of Tables (Continued)

LIST OF FIGURES

DEFINITION OF SYMBOLS

A, a, b	Empirical coefficients
D	Soil moisture diffusivity coefficient
$\overline{D}$	Weighted mean diffusivity
$\overline{D}^o$	Intrinsic weighted mean diffusivity
DOH	Deuterium hydroxide
E_a	Arrhenius activation energy
ΔF^*	Free energy of activation
g	Gravitational constant
ΔH^*	Heat of activation
h	Planck's constant
K	Rate coefficient
k	Intrinsic permeability
ln	Natural logarithm
log	Logarithm to the base 10
M	Gram-molecular weight
N	Avogadro's number
n	Emperical exponent
P	Pressure
P_w	Moisture content percent by weight
Q	Total volume of flow
q	Volume of flow per unit area
R	Universal gas constant
S	Sorptivity coefficient
S^o	Intrinsic sorptivity
ΔS^*	Entropy of activation
T	Absolute temperature
t	Time
V	Molar volume
v	Volume of flow per unit area per unit time
$\overline{v}$	Average velocity of flow
β	Regression coefficient
γ	Surface tension
$\triangle$	Increment
η	Dynamic viscosity
θ	Moisture content, proportion of volume
θ_o	Initial moisture content
θ_s	Moisture content at saturation
λ	Soil moisture conductivity coefficient
μ	Microns
π	3.1416
ρ	Density
ρ_B	Soil bulk density
τ	Soil moisture suction
ϕ	Soil moisture potential
ψ	Soil moisture potential excluding potential due to position in gravitational field
∇	Gradient operator

INTRODUCTION

Water moves in soil in response to potential gradients. The basic
equation for this movement is the generalized flow equation:

$$v = -K\nabla\phi \qquad (1)$$

in which v is volume of water passing through a unit area in unit
time, K is the conductivity coefficient, ∇ is the gradient operator
(vector), and $\nabla\phi$ is the potential gradient.

The conductivity coefficient, K, is a constant for any fixed
soil-water system, but will vary with changes in moisture content,
temperature, structure, and the other variables in the system. This
equation forms the basis of all recognized moisture flow equations.

That temperature influences soil moisture movement rates has long
been recognized. It has generally been assumed that the temperature
effect was due to the temperature dependence of the viscosity of water,
and that temperature effects could be accounted for by corrections
based on the viscosity of pure free water at the temperature of interest.
Equation (1) has been modified as follows to account for temperature
effects:

$$v = - \frac{k}{\eta}\nabla\phi \qquad (2)$$

in which k is called permeability and η is the viscosity of pure
free water at the ambient temperature. Various forms of equation (2)
have been applied with a fair degree of success to saturated flow

problems. However, recent studies indicate that viscosity of soil water, especially strongly adsorbed water, may be greater than that of free water and, consequently, the temperature effects may be different. This increased viscosity of adsorbed water may be responsible for some of the anomalies encountered in attempts to apply conventional fluid mechanics laws to soil moisture flow.

In general, the stronger the bonds between molecules of a liquid, the greater is the effect of temperature changes on the fluid properties of that liquid. Soil water, being subject to adsorptive forces of the soil solids, can be expected to exhibit greater temperature dependence of flow properties than does free water. In saturated soil, especially one with large pores, a large portion of the water is not subject to strong attractive forces and the effects of temperature may not be appreciably greater than indicated by equation (2). In unsaturated soil, the forces between water molecules are greater than they are in free water, and these forces can be expected to increase as soil moisture tension increases. As a result, the effects of temperature on fluid properties would be greater in unsaturated soil than in saturated soil and the temperature correction contained in equation (2) may not be adequate.

LITERATURE

Early developments

King (1892) was among the first to study the effects of temperature on soil moisture-holding capacity and soil moisture movement. In his studies of water levels in wells he noted that during the summer these levels rose during the day and subsided at night. To determine the cause of these oscillations, he filled a water-tight cylinder, 6 feet deep and 30 inches in diameter, with soil and added water until it stood about 1 foot deep in a small well in the center of the cylinder. Water stage records of the level in this well showed diurnal fluctuations as great as 1.8 inches. He placed thermometers in the cylinder and found that changes in water level followed closely the changes in soil temperature. To prove that this covariance was not coincidental he sprayed cold water on the cylinder on a hot afternoon when the water level was rising. This caused the water level to halt and then start to fall. King inferred that the water-holding power of soil is inversely related to temperature and that the magnitude of the temperature effect appeared greater than he would expect to attribute to the effect of temperature on surface tension.

King (1892) also reported observations of the influence of temperature on percolation rates. While attempting to determine the effects of salt on percolation rate he found that variations in temperature so greatly affected his measurements that precise temperature control was necessary to obtain concordant results. He reported the following

measurements of the effects of temperature on water flow rates in coarse
sand:

Temperature	^{o}C	9.0	12.6	23.8	32.5
Flow rate	grams/min	6.15	7.05	9.01	10.54.

King offered no explanation for these differences other than that
the coefficient of expansion of the walls of the apparatus differed from
that of the sand but he admitted this could not account entirely for the
observed differences in flow rates. It was Briggs (1897) who explained
that the differences were due to viscosity changes. He pointed out that
the ratio of the rate of flow at 32.5^{o}C to that at 9.0^{o} is 1.71 while
the ratio of water viscosity at 9.0^{o}C to that at 32.5^{o} is 1.77, indicating
that the differences in flow rate could be accounted for almost entirely
by viscosity changes.

Briggs (1897) introduced several important concepts of the mechanics
and temperature dependence of soil moisture retention and movement. The
well-known generality of three classes of soil water: gravitational,
capillary, and hygroscopic was originally proposed by Briggs. Gravita-
tional water is the water that drains from a saturated soil until the
gravitational force is balanced by surface tension forces. As soil
moisture content of the soil decreases, the air-water interfacial area
and the curvature increases, creating retentive forces in opposition to
the gravity force. Briggs considered the capillary water to be a contin-
uous film in which, at equilibrium, the resultant forces of gravitation
(weight of the water) and surface tension were zero at all points, and
therefore, surface tension forces must increase with increasing height
above a free water surface. In uniform soil, then, moisture content will
vary inversely with height.

Because surface tension is inversely related to temperature, moisture content of unsaturated soil must decrease with increasing temperature in order to maintain surface tension forces sufficient to counteract those of gravity. Briggs cites King's (1892) study of the fluctuations of the water level in the tank of soil in support of this hypothesis. King found that the height of the water table was positively related to soil temperature or, in other words, the moisture-holding power of the soil above the water table was inversely related to temperature. Briggs attributed the inverse relation between moisture content and temperature to the temperature dependence of surface tension.

Briggs (1897, p. 19-20) described capillary flow as the adjustment of water between points of unequal pressure and stated:

> The rate at which this adjustment of water between two capillary spaces will take place depends upon the viscosity of the connecting film, the surface tension, and the difference in curvature of the films. The viscosity of the connecting film does not in any way interfere with the final adjustment of the water, but it retards to a greater or less degree the establishment of equilibrium.

Discussing the temperature dependence of water viscosity and surface tension, Briggs implied that both the driving force and the rate of water movement in response to the driving force are affected by temperature.

Although the potential concept as introduced by Buckingham (1907) did not explicitly include temperature effects, it was a significant contribution to capillary flow theory. By analogy to Ohm's law for electrical current and Fourier's laws of heat flow, Buckingham proposed for moisture flow in unsaturated soil:

$$v = -\lambda \frac{\partial \psi}{\partial x} \tag{3}$$

in which v is the moisture flux in the x direction at a given point; λ is a conductivity coefficient dependent on soil moisture content, and ψ is the soil moisture potential, an energy term analogous to voltage or temperature. Equation (3) is also analogous to Darcy's law for saturated flow of water through sand but Buckingham did not discuss this point. By proposing soil moisture potential, whose space gradient is (by definition) the driving force, Buckingham provided a simple equation for unsaturated soil moisture movement.

Bouyoucos (1915) also studied the effects of temperature on soil moisture retention and movement. As did King, he found moisture content inversely related to temperature to such a degree that he concluded that factors in addition to surface tension were involved. He measured percolation rates in six soils with differing textures (sand, sandy loam, silt loam, clay loam, clay, and muck) at 0°, 10°, 20°, 30°, 40°, and 50^oC. Only in the sand was the conductivity at the various temperatures proportional to water viscosity. In all the other soils, conductivity increased with temperature up to a maximum at about 30^oC and then decreased with further increases in temperature. In the silt loam and clay loam the conductivity was about the same at 50^oC as it was at 10^oC but the conductivity of the clay was lower at 50^oC than at 0^oC. These results led him to conclude it would be futile to attempt to apply Poiseuille's capillary tube flow equation to such data because "the soil material is dynamic, not static." He explains the results with the hypothesis that increased temperature causes the colloidal material to swell and tend to close the water-conducting pores.

From Stokes' equation of the motion of a particle falling through a fluid, Gardner (1919) ingenuously derived an equation for unsaturated flow which was similar to Buckingham's but included viscosity:

$$v = \frac{k}{\eta} \frac{dp}{dx} \tag{4}$$

in which v is the velocity of the soil particle relative to the fluid, k is dependent on the size of the soil particle, η is viscosity, and $\frac{dp}{dx}$ is the pressure gradient. Gardner did not discuss the implications of this equation relative to temperature dependence of unsaturated flow.

Combining the equation of capillary rise with Poiseuille's equation of flow in capillary tubes, Washburn (1921) derived the following equation for one-dimensional infiltration of liquid into porous materials under negligible pressure:

$$q = A \left(\frac{\gamma \cos\theta}{\eta}\right)^{\frac{1}{2}} t^{\frac{1}{2}} \tag{5}$$

in which q is the volume of fluid absorbed per unit area in time t, A is a constant for the porous material, γ is the surface tension of the fluid, ϕ is the wetting angle, and η is viscosity. Washburn included surface tension and viscosity in the equation to separate the fluid properties from the properties of the porous solid; he did not discuss temperature effects specifically. Forms of equation (5) have been applied to soil by Swartzendruber et al. (1954) and Phillip (1957) but without specific reference to temperature effects. Jackson (1963) utilized modifications of equation (5) in his study of temperature dependence of infiltration rates, which will be discussed in a following section.

In studies of upward movement of moisture from a water table, Moore (1939) found that a drop in temperature always resulted in an increased rate of water intake. This he attributed to the effect of temperature on moisture potential. The potential at a given moisture content in unsaturated soil decreases with decreasing temperature, resulting in a steeper potential gradient and, therefore, increased flow rates. He stated that variations in temperature can cause fluctuations in moisture content and moisture movement that may vitiate the accuracy of many types of soil moisture studies.

In another study Moore (1940) investigated the effects of temperature on potential, retention, and infiltration rate of water in soils ranging in texture from sand to clay. Due to hysteresis effects and other experimental difficulties, he found no reliable relations between temperature and potential at constant moisture content, nor between temperature and moisture content at constant potential. He did find a significant inverse relation between temperature and moisture content of the surface 10 inches of soil 6 days after irrigation, perhaps due to greater moisture mobility at higher temperatures induced by the inverse relation between temperature and viscosity. Infiltration rates at 1 minute after irrigation tended to increase with temperature from 5° up to $35^{\circ}C$ and then declined in all four soils tested. This, too, may be due to the inverse viscosity-temperature relation but the maximum at 35° suggests influence of other factors.

Diffusivity equations

When Buckingham (1907) proposed his potential theory of moisture movement he presented the following equation as equivalent to equation (3):

$$v = -\lambda \frac{\partial \psi}{\partial \theta} \frac{\partial \theta}{\partial x} \tag{6}$$

in which v is flux of water in the x direction at a given point, λ is the capillary conductivity coefficient dependent on moisture content, θ is the volumetric moisture content (volume of water per unit volume of soil), $\frac{\partial \psi}{\partial \theta}$ is the rate of change in potential with change in moisture content and is a function of moisture content, and $\frac{\partial \theta}{\partial x}$ is the concentration gradient of moisture in the x direction.

Childs and Collis-George (1948) proposed a new coefficient:

$$D = \lambda \frac{\partial \psi}{\partial \theta} \tag{7}$$

called the soil moisture diffusivity coefficient which is a function of moisture content, being a product of two functions of moisture content. It is generally assumed to be a single-valued function of θ for either a wetting process or a drying process but, due to hysteresis effects, not for a combination of the two. It may be considered the coefficient of flow in response to a concentration gradient because substituting D into equation (6) yields:

$$v = -D \frac{\partial \theta}{\partial x} \tag{8}$$

Combining equation (8) with the continuity equation $\frac{\partial \theta}{\partial t} = -\frac{\partial v}{\partial x}$ yields:

$$\frac{\partial \theta}{\partial t} = \frac{\partial}{\partial x}(D \frac{\partial \theta}{\partial x}) \tag{9}$$

This is known as the soil moisture diffusion equation and has received a great deal of attention in recent years. Klute (1952) devised a numerical method for solving equation (9) for dynamic moisture movement in soil. Several other soil physicists have devised and applied various methods of solving and using equation (9), but only a few have dealt with the temperature dependence of soil moisture diffusivity.

Gardner (1959) measured diffusivity coefficients at saturation and at air-dry moisture contents on five soils of different textures. In all soils diffusivity at saturation increased with temperature but the temperature dependence of diffusivity at air-dry moisture content varied according to the clay content of the soil. Air-day diffusivity increased with increasing temperature in the two sandy loams; it was essentially independent of temperature in the loam containing 16 percent clay; and decreased with increasing temperature in the loam containing 23 percent clay and in the Chino clay soil.

Gardner also determined the temperature dependence of the weighted mean diffusivity $\overline{D}$ which he defined by:

$$v = (\theta_s - \theta_o) \sqrt{\frac{\overline{D}}{\pi t}} \tag{10}$$

in which v is the intake rate per unit area at time t, θ_s is volumetric moisture content at saturation, and θ_o is the initial moisture content. $\overline{D}$ increased with increasing temperature in one sandy loam, and increased at a slightly lower rate in the other soils. Gardner concluded that the viscosity effect is predominate near saturation but at lower moisture contents the effect of temperature on suction becomes important and may, in some cases, exceed the viscosity effect. The hysteresis effect may

exceed the temperature effect and, for many cases, he considered it acceptable to assume diffusivity independent of temperature.

Stewart (1962) measured diffusivity coefficients in a kaolinitic silty clay loam at temperatures ranging from 8° to 40°C. Diffusivity increased with temperature at all moisture contents. Stewart corrected these coefficients for viscosity by multiplying them by the ratio of free water viscosity at their respective temperatures to the viscosity at 20°C. The corrected diffusivities were virtually independent of temperature but tended to increase with temperature at high moisture contents and decrease with increasing temperature at low moisture contents.

Stewart (1962) discussed various aspects of temperature dependence of soil moisture diffusivity. From the data of Taylor and Stewart (1960), he infers that the value of $\frac{\partial \psi}{\partial \theta}$ decreases with increasing temperature and as water content decreases the effect of temperature on $\frac{\partial \psi}{\partial \theta}$ increases. Thus, while increasing temperature would tend to increase the conductivity (λ) component of diffusivity due to the inverse viscosity-temperature relation, its effect on $\frac{\partial \psi}{\partial \theta}$ would tend to decrease diffusivity, especially at lower moisture contents. Stewart also pointed out that the heat evolved during water sorption by soil is a source of error that is difficult to correct. The temperature rise at the wet front may affect viscosity and potential gradients significantly.

Jackson (1963) studied the effects of temperature on moisture diffusivity relations in two loam soils and a silty clay. Diffusivities were 2 to 3 times greater at 42.5° than at 5°C but he observed no measurable differences in the temperature dependence of diffusivities at different moisture contents. Assuming that diffusivities at all moisture

contents vary with temperature in the same manner, he proposed that the temperature dependence of the weighted mean diffusivity ($\overline{D}$) would hold true for diffusivities at all moisture contents. Using Gardner's equation (10), he calculated $\overline{D}$ at 5 different temperatures for the three soils. After Philip (1957), he defined intrinsic weighted mean diffusivity $\overline{D}^O$ by the equation:

$$\overline{D}^O = \frac{\eta}{\gamma} \overline{D} \tag{11}$$

Calculating $\overline{D}^O$ for all 5 temperatures using the values for viscosity (η) and surface tension γ given by Dorsey (1940), he found it to be unrelated to temperature in all 3 soils tested and concluded that the temperature dependence of soil moisture diffusivity is dominated by the temperature dependence of the ratio of surface tension to viscosity.

In comparing Jackson's results with those of Stewart (1962) one should notice that the temperature dependence of surface tension is small compared to that of viscosity and therefore the inclusion of surface tension in the correction factor would have a minor effect.

Activation energy and viscosity

The activation energy concept has recently been borrowed from chemical kinetics and applied to soil moisture movement by several soil scientists. In its simplest form, activation energy may be defined by the Arrhenius equation (Frost and Pearson, 1953, p. 23):

$$E_a = RT^2 \frac{d \ln K}{dT} \tag{12}$$

in which E_a is the Arrhenius activation energy, K is a chemical rate constant or any other accurate parameter of molecular reaction, R is the

universal gas constant, and T is absolute temperature. The temperature dependence of a large number of simple chemical reaction rates can be characterized by equations of this type. E_a is considered the energy barrier which must be surmounted for a reaction to take place. In the case of evaporation from a liquid surface it is the energy of vaporization. In the case of viscous flow it is N times the average energy required for a molecule to move out of an equilibrium position far enough to be pulled into another equilibrium position, N being the number of molecules per mole.

A common method of calculating E_a is to plot log K as a function of $\frac{1}{T}$ and measure the slope of the resulting line. Equation (12) can be restated as follows to give E_a as proportional to that slope:

$$E_a = -2.303R \frac{d \log K}{d(\frac{1}{T})} \tag{13}$$

Biggar (1956) was probably the first to apply the activation energy concept to soil moisture movement. He measured rates of water uptake of Millville silt loam in horizontal cylinders at 10°, 20°, 30°, and 40^oC. The data followed closely the equation:

$$q - St^{\frac{1}{2}} \tag{14}$$

in which q is the cumulative water uptake per unit area in time t and S is a constant coefficient presently known as sorptivity. Assuming S to be a bona fide rate constant, he plotted log S as a function of $\frac{1}{T}$ and determined E_a according to equation (14), obtaining values of E_a ranging from 1.0 to 2.9 kilocalories per mole (Biggar and Taylor, 1960). The validity of the assumption of S being a rate constant will be discussed in a following section.

Wiegand and Taylor (1960) used the activation energy concept in their studies of the temperature dependence of the drying of soil columns. They measured rates of evaporation from columns of Millville silt loam under carefully controlled initial and boundary conditions at temperatures ranging from 12.7° to 37.7°C and found that, during the first 50 hours or so, cumulative evaporation followed closely the equation:

$$Q = at^{0.92} \tag{15}$$

in which Q is the cumulative evaporation at time t and a is a coefficient dependent on temperature but independent of time. Rates of evaporation from the warmer columns followed equation (15) for about 50 hours and then declined abruptly. Rates in the cooler columns followed equation (15) for a longer period of time, up to about 180 hours, and then also declined abruptly. Taking the cumulative evaporation at 20 hours as the rate constant (K of equation 12) they calculated activation energies of 6.9 ± 2.3 kilocalories per mole for those columns which were 31 centimeters high and had a water table at the bottom, and 9.3 ± 1.4 for those columns which were 18 centimeters high and had no water table at the bottom. These activation energies are intermediate between E_a for viscosity of water (about 4 kilocalories per mole) and the latent heat of vaporization which is about 10.5 kilocalories per mole, indicating a temperature dependence greater than that of normal viscous flow but an apparent energy barrier somewhat less than that of vaporization.

Low (1960) measured rates of flow of water through saturated Na-bentonite under constant pressure difference at various temperatures ranging from 25° to 36°C. Plotting the logarithms of these rates as functions of $\frac{1}{T}$, he used an equation similar to equation (13) to calculate

activation energies of saturated flow. The calculated activation energies varied from 3835 to 4356 calories per mole, essentially the same or slightly greater than that for the flow of normal water, which Low states is 3862 calories per mole in the 25° to 38°C range. Low called attention to Carmen (1939), Rosenqvist (1959), and others whose investigations suggest unusually high viscosity of water adjacent to clay surfaces, and proposed that soil water viscosity relations might be studied by means of the activation energy concept in the more sophisticated form embodied in Eyring's theory of absolute reaction rates. Eyring's theory will be discussed in a following section.

Anderson et al. (1963) determined apparent activation energies for water movement in liquid and vapor phases in a rather unusual way, making use of the temperature fluctuations associated with an advancing wetting front. They recorded the temperature at two points in horizontal soil columns during infiltration of water and assumed that the first detectable rise in temperature indicated the arrival of water vapor at the measuring site and that the peak temperature occurred at the time liquid water reached the monitored site. In this way they measured velocity of both vapor and liquid during infiltration at ambient temperatures varying from 15° to 41°C in three soils: Arizona bentonite, a sandy loam, and a muck soil. Activation energies were calculated separately for vapor movement and liquid movement by plotting $\ln \bar{v}$ as a function of $\frac{1}{T}$ and using the following modification of equation (13):

$$E_a = -R \frac{d \ln \bar{v}}{d(\frac{1}{T})} \tag{16}$$

in which $\bar{v}$ is the average velocity of vapor or liquid between two fixed points (1 centimeter apart) in the soil column. Apparent activation

energies for liquid movement were 6.0, 6.1, and 4.3 kilocalories per mole

for Arizona bentonite, the muck soil, and the sandy loam, respectively.

These activation energies were all significantly greater than that of

normal water which has an E_a of viscosity of about 3.8 kilocalories per

mole. The authors attribute the additional energy to the extension of

the air-water interface.

Activation energy for vapor movement was 9.7 kilocalories per mole

for the Arizona bentonite and 9.8 kilocalories per mole for the muck

soil. These values are essentially the same as the energy of vaporiza-

tion of water. The authors concluded that extension of the liquid inter-

face and viscous flow were the processes limiting liquid movement and

that vaporization at the wetting front limited the rate of vapor movement.

The activation energy approach appears to be a promising method of

studying soil moisture movement but results of such studies reported to

date appear to be in conflict with the findings of those such as Rosenqvist

(1959) and Kunze and Kirkham (1961) who have found that diffusion coeffi-

cients of deuterium hydroxide much lower in soil water than in free water.

This is indicative of higher viscosity of soil water compared to free

water because, according to Wang et al. (1953), viscosity is proportional

to absolute temperature divided by the self-diffusion coefficient. If

the diffusion coefficient of DOH in soil-water is the same as the self-

diffusion coefficient of soil water, the data of Kunze and Kirkham (1961)

indicate a fourfold increase in soil water viscosity in an unsaturated

clay loam soil at 20 centimeters moisture tension. The data of Rosenqvist

(1959) for marine clay containing 10 percent moisture indicate soil-water

viscosities more than 100 times greater than free water. Wu (1964)

studied the nuclear magnetic resonance of soil water and found further

evidence that adsorbed water is much more viscous than ordinary water.

None of the studies of activation energy reported to date substan-
tiate the probability of higher viscosity near water-soil interfaces.
However, only in Low's (1960) study was the temperature dependence of
the conductivity separated from that of potential gradients. In the
other studies some form of diffusivity was used as the rate constant and,
as pointed out by Stewart (1962), it is quite possible that a high degree
of temperature dependence of soil moisture conductivity could be compen-
sated by a large inverse relation between temperature and potential
gradient, resulting in apparent viscosities of soil water essentially
the same as those of free water. The activation energies obtained by
Low (1960) in saturated bentonite are probably not significantly greater
than free water viscosity but, since he was dealing with saturated flow,
perhaps the bulk of the water moving through the system was far enough
from the clay surfaces that its viscosity was not significantly affected.
In an unsaturated system, the bulk of the flow would occur closer to the
clay surfaces and could be expected to exhibit a greater activation
energy.

THEORY

Glasstone et al. (1941) state that both diffusion and viscosity can be treated by means of Eyring's theory of absolute reaction rates and propose the following theoretical equation for viscosity:

$$\eta = \frac{Nh}{V} \, e^{\triangle F*/RT} \tag{17}$$

in which η is viscosity, h is Planck's constant, N is Avogadvo's number, V is the molal volume of the liquid, and $\triangle F*$ is the standard free energy of activation per mole. In logarithmic form, equation (17) may be written:

$$\ln \eta = \ln N H - \ln V + \frac{\triangle F*}{RT} \tag{18}$$

Replacing $\triangle F*$ with $\triangle H* - T \triangle S*$ yields

$$\ln \eta = \ln N H + \frac{\triangle H*}{RT} - \frac{\triangle S*}{R} - \ln V \tag{19}$$

$\triangle H*$ is heat of activation and $\triangle S*$ is entropy of activation. Multiplying both sides of equation (19) by R and differentiating with respect to T yields:

$$R \, \frac{d \ln \eta}{dT} = - \frac{\triangle H*}{T^2} + \frac{1}{T} \frac{d \triangle H*}{dT} - \frac{d \triangle S*}{dT} - R \, \frac{d \ln V}{dT} \tag{20}$$

If the last three terms in equation (20) are considered negligible the equation may be written:

$$\triangle H* = - RT^2 \, \frac{d \ln \eta}{dT} \tag{21}$$

which is equivalent to the Arrhenius equation (12), $\triangle H*$ being

analogous to E_a and $(-d \ln \eta)$ being analogous to $(d \ln K)$. This equation has been found to be in excellent agreement with experiment for many liquids. However, for water and other associated liquids, neither $\triangle S^*$ nor $\triangle H^*$ is independent of temperature and equation (21) is a rather poor approximation for such liquids. The inconstancy of $\triangle S^*$ and $\triangle H^*$ is due to the quasi-crystalline structure of water which varies with temperature (Grunberg and Nissen, 1949).

$(\triangle H^* - T\triangle S^*)$ was substituted for $\triangle F^*$ in equation (18) in order to replace a temperature dependent term with two terms assumed to be independent of temperature. This substitution apparently produced the desired results for many liquids but not for water. Table 1 shows values of E_a for water calculated by Arrhenius equation (13). These values change appreciably with temperature. This means that, for water viscosity, E_a is not equivalent to $\triangle H^*$ in equation (21) because the derivation of that equation assumes $\triangle H^*$ independent of temperature.

Table 1. Free water viscosity, its Arrhenius activation energy (E_a) and its free energy of activation ($\triangle F^*$) at 10° to $50^o C$

Temperature °C	Viscosity millipoises	E_a	$\triangle F^*$
		kilocalories	per mole
10	13.08	4.57	2.30
15	11.40	4.34	2.26
20	10.05	4.16	2.22
25	8.94	4.00	2.19
30	8.01	3.87	2.16
35	7.22	3.74	2.13
40	6.56	3.65	2.11
45	6.00	3.56	2.09
50	5.49	3.47	2.07

Several workers have noted that a curve rather than a straight line results when the logarithms of viscosity or a variable dependent on viscosity of associated liquids is plotted as a function of $\frac{1}{T}$. Litowitz (1952) proposed the equation

$$\eta = Ae^{a/RT^3} \tag{22}$$

in which A and a are empirical coefficients dependent on the liquid but independent of temperature for such liquids as water, glycerol and some alcohols. Plotting the logarithms of viscosity of any of these liquids as a function of $\frac{1}{T^3}$ results in a straight line.

Innes (1956) proposed another alternative:

$$\eta = AT^n e^{B/T} \tag{23}$$

A, n, and B being empirical coefficients dependent on the liquid but not on temperature.

Because the temperature dependence of $\triangle F^*$ of water viscosity is not satisfactorily accounted for by substituting $\triangle H^* - T\triangle S^*$, it is proposed that the following empirical equation be used instead:

$$\triangle F^* = aRT = bRT^{-2} \tag{24}$$

in which a and b are temperature-independent empirical coefficients. Values of $\triangle F^*$ for water viscosity calculated directly from a rearrangement of equation (18) are presented in Table 1. Fitting equation (24) to these data yields a value of 1.465 for coefficient "a" and 5.93×10^7 for coefficient "b". Combining equations (18) and (24) gives:

$$\ln \eta \; V = \ln N \; h + a + bT^{-3} \tag{25}$$

When the values of a and b just given are substituted into this equation, it is accurate to at least 3 significant figures for water viscosity in the 10° to 50^oC temperature range. Differentiating equation (25) with respect to T^{-3} yields:

$$\frac{d \ln \eta V}{d(T^{-3})} = b \qquad (26)$$

If $\ln \eta V$ of free water is plotted as a function of T^{-3}, the result is a straight line whose slope is b. While perhaps lacking in physical significance in itself, the coefficient b provides a link between Arrhenius's E_a and Eyring's ΔF^* for water viscosity. The relation between E_a and b is shown in Appendix V.

In the present study, Buckingham's equation (3) for flow in unsaturated soil will be assumed to be valid. The temperature dependence of the capillary conductivity coefficient (λ) will be attributed to the temperature dependence of water viscosity and density as implied in the definition of intrinsic permeability (k) by Richards (1952):

$$k = \frac{\lambda \eta}{\rho g} \qquad (27)$$

k is intrinsic permeability independent of fluid properties, ρ is density of the fluid and g is acceleration due to gravity. Rearranging equation (27), substituting $\frac{M}{V}$ for ρ, and converting to natural logarithms yields:

$$\ln \lambda = \ln k g M - \ln V \eta \qquad (28)$$

M is gram-molecular weight of the fluid. Combining equations (25) and (28) gives:

$$\ln \lambda = \ln k g M - \ln N h + a + bT^{-3} \qquad (29)$$

Differentiating equation (29) with respect to (T^{-3}) yields:

$$\frac{d \ln \lambda}{d(T^{-3})} = -b \qquad (30)$$

This equation allows us to use values of λ determined at various temperatures to evaluate the coefficient b. This leaves two unknowns in equation (29): a and k. The theory presented here does not offer a means of evaluating the two separately so that neither intrinsic permeability nor absolute values of ΔF^*, η, or ρ can be determined for soil water unless one or more arbitrary assumptions are made. Equation (30) does provide a simple parameter of temperature dependence of water viscosity with which free water can be compared with soil water. As already stated, the coefficient "b" is 5.93×10^7 for free water in the 10° to 40^oC range.

SCOPE

This study involves the determination of capillary conductivity coefficients in the tensiometer range of moisture stress at temperatures ranging from 12°C to 40°C in three soils. Potential gradients were determined by means of tensiometers, it being assumed that no gradients other than those caused by matric potential differences were present. Values of λ at four different temperatures were determined as functions of potential. Values of λ as functions of moisture content and temperature were derived from these by use of experimentally determined values of potential as a function of moisture content and temperature. The temperature dependence of these latter values of λ was determined by means of linear regression analyses in which the coefficient "b" of equation (30) was evaluated for various soils at various moisture contents.

METHODS AND MATERIALS

The apparatus (Figures 1 and 2) consists of a lucite cylinder, 88 mm inside diameter and 101 mm outside diameter, in which six tensiometer cups are placed at 50 mm intervals. These cups[1] are 9 mm in diameter and 110 mm long, extending the full width of the lucite cylinder and anchored at both ends with epoxy cement. Porous plates at each end are held against the soil at constant pressure by spring loading. The sliding joint illustrated in Figure 1 is machined for a snug yet free-sliding fit. All parts of this apparatus, other than the ceramic cups and plates and the metal hardware are made of lucite. Lucite parts were welded together with methylene chloride. Ceramic parts were bonded to lucite parts with epoxy cement but later, after the apparatus was constructed, Silastic[2] was found to be better for this purpose and was used for subsequent repairs.

Three different soils were used in this study: Millville silt loam, a clay loam from the subalpine zone of the Wasatch Plateau in central Utah, and another clay loam from the mountain brush zone on the west slope of the Wasatch Plateau. All of these soils are calcareous and the latter two are high in organic matter content and highly aggregated under natural conditions. The subalpine soil contains about 7 percent more clay than the mountain brush soil. These soils were air-dried

---

[1]Tensiometer cups and porous plates are ceramic units with air entry values of 1 bar, obtained from Lark Instruments, Riverside, California.

[2]Silastic RTV 731 - a silicon rubber sealant manufactured by Dow Corning Corporation, Midland, Michigan.
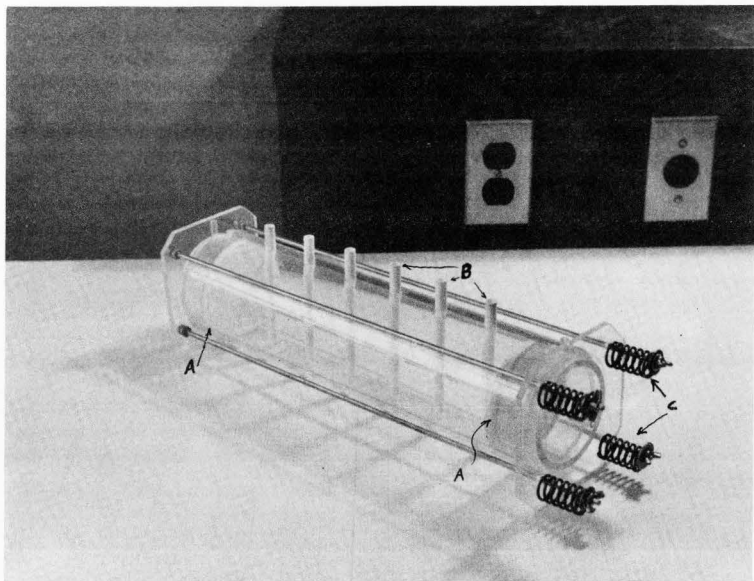
Figure 1. Soil moisture conductivity cylinder showing: A. porous end
plates, B. tensiometer cups, and C. springs to keep soil in
contact with the ceramic plates.
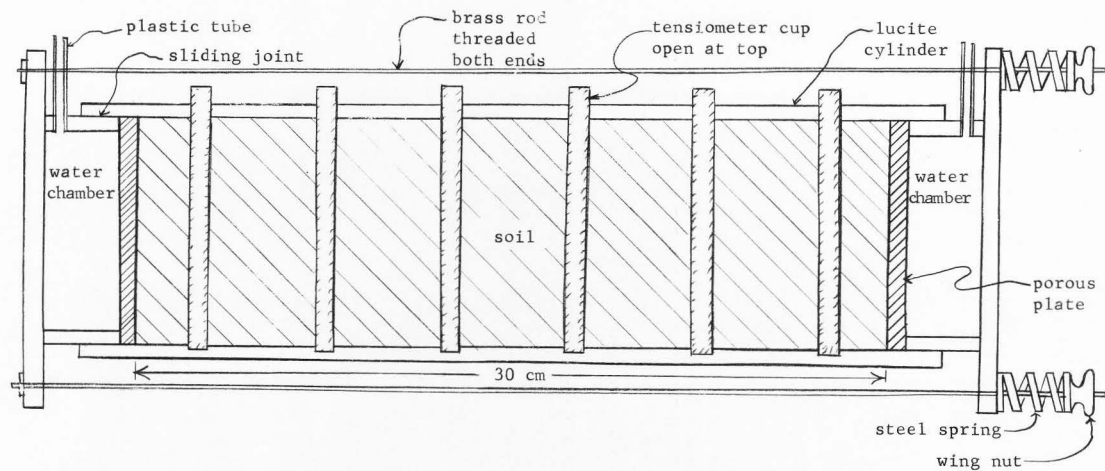
Figure 2. Diagrammatic view of soil moisture conductivity cylinder

and passed through a 2 mm sieve before being used in this study.

Soils were carefully packed in the cylinders just described. Four cylinders were used: one containing Millville silt loam, one containing a mountain brush zone soil, and two containing a subalpine soil at differing bulk densities. The uniformity of soil packing was checked visually by observing the soils appearance through the cylinder walls and also by the following weighing procedure. The empty cylinder, with its water chambers fixed in the position they would occupy after the cylinder was filled with soil, was weighed and its center of gravity determined. The cylinder was then filled with air-dry soil using a tremie and tapping the sides of the cylinder continually throughout the filling operating. The cylinder was again weighed to determine the weight of soil added and its center of gravity determined. The center of gravity of the soil was then calculated, using the principle of moments, and if it deviated measurably from the midpoint between the two porous plates the soil was removed and repacked. All cylinders had to be repacked at least once and one cylinder was repacked three times before a satisfactory position of the center of gravity was obtained. Although deviations in bulk density could escape detection by these methods, these deviations are minor and tend to moderate after a few months in the cylinder under moist conditions.

After the cylinders were satisfactorily filled with soil, the chambers at each end were filled with water and the soil slowly wetted as water flowed through the porous plates. Due to high impedence of the plates, wetting of the soil took place under tensions at about 50 to 100 cm of water.

These four cylinders were placed in an air-bath (Figure 3) which could be controlled to $\pm$ 0.05°C. This air-bath was an enclosed air space above the surface of a thermostatted water bath. The temperature of the air was regulated by adjusting the temperature of the water bath. A small electric fan kept the air in motion. The air was saturated, or nearly so, with water vapor from the free water surface, thus greatly reducing the possibility of evaporation from the soil-water systems.

The tensiometer cups were filled with water and connected to mercury manometers. These four groups of six manometers can be seen in Figure 3. Water reservoirs were connected with capillary glass tubing to the water chambers of the soil cylinders, and provision was made to introduce air bubbles into these capillary tubes so that the velocity of flow in the tubes, and thereby the water flux into and out of the soil, could be measured. The filtering flasks in Figure 3 are the water reservoirs, the capillary bubble tubes are on top of the insulated bath, and the glass stopcocks serve to introduce bubbles into the capillary tubes.

Water tension within the chambers was regulated by mercury cartesian manostats which controlled the air pressure in the filtering flasks. These manostats were connected to a small vacuum pump capable of maintaining a vacuum of about 60 cm of mercury at the elevation of Utah State University (4,500 feet, M.S.L.). The soil system itself remained at atmospheric pressure.

Provision was also made to transfer water from the flasks at the outlet side to the flasks at the inlet side so that the effluent water could be recirculated through the soil system, thereby minimizing leaching.
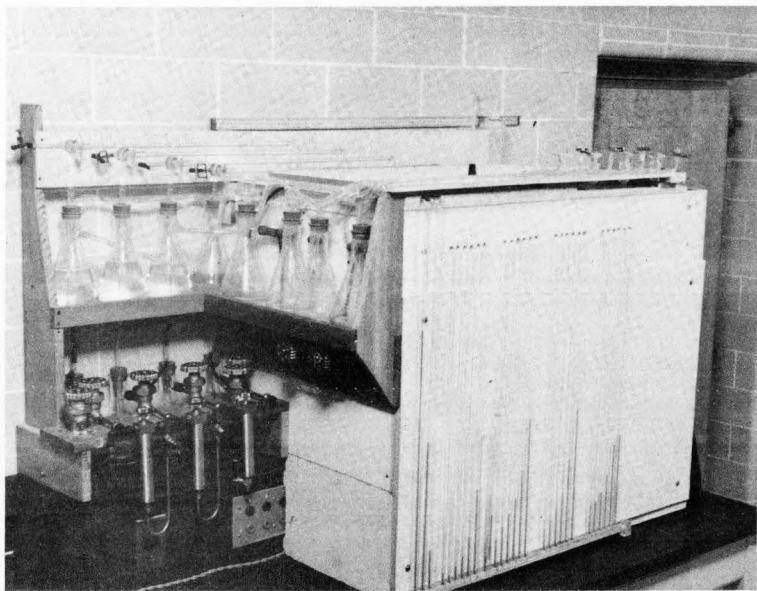
Figure 3. Controlled temperature bath with manometer board and flow rate
tubes attached. Filter flasks serve as water reservoirs. The
three metal cylinders in the lower left are cartesian manostats.

The procedure used to determine capillary conductivity coefficients is as follows: the air bath temperature was maintained constant at one of the four temperatures; 12.0^o, 20.0^o, 30.0^o, or 40.0^oC. A constant low tension was maintained in the water chamber on the inlet side of the soil cylinder and a constant higher tension was maintained on the water in the chamber on the outlet side. Inflow rates and soil moisture tensions were monitored and steady state conditions were assumed to exist when no further changes in these were observed. Originally it was planned to measure outflow rates and require that outflow equal inflow for steady state but it soon became apparent that diffusion of gas through the porous plate and the erratic development of minute leaks under the high vacuum conditions on the outlet side spoiled the accuracy of the bubble tube method of measuring flow. Only at the lower tensions on the outlet chamber were usable outflow measurements obtained.

When steady state was attained, flow rates and moisture tension distribution were recorded. For any given cylinder the tension gradient at any specified tension within the range of measurement can be determined by plotting soil moisture tension as a function of position in the cylinder and measureing the slope of the fitted curve at the tension of interest. An example of tension plotted as a function of position in the dashed curve in Figure 4. If tension distribution is plotted on semi-log graph paper, the fitted curve is equivalent to the solid curve in Figure 4, which was plotted from the same data as the dashed curve. Such a curve is easier to fit and its slope at any apecified tension (τ) can be converted to tension gradient by the simple relation:

$$\frac{d\tau}{dx} = \tau \frac{d \ln \tau}{dx} \tag{31}$$
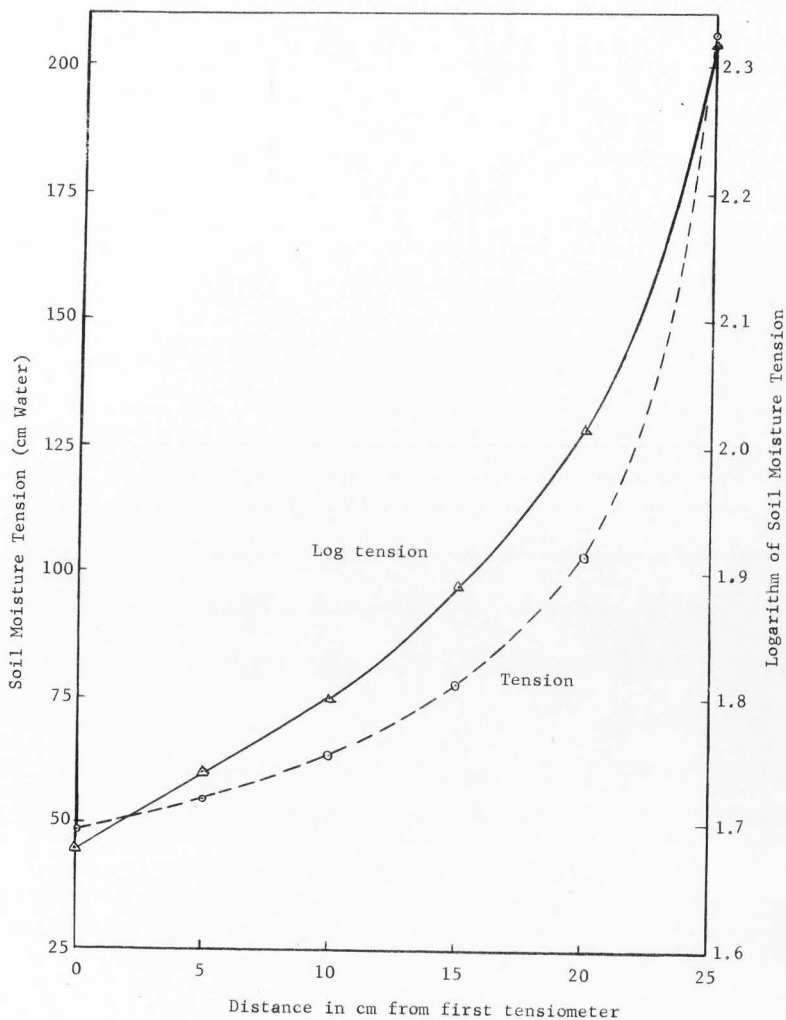
Figure 4. Soil moisture tension as a function of position compared with
           logarithm of tension as a function of position. Read on
           22 January 1963, Cylinder A (subalpine soil).

Tension gradients can be measured more accuratedly this way than by measuring slopes of curves fitted to arithmetic tension distributions. The logarithmic method was used for all tension gradient determinations reported in this paper.

If tension gradient is the only driving force involved, Buckingham's equation (3) can be rewritten:

$$\lambda = \frac{v}{\tau} \frac{dx}{d \ln\tau} \tag{32}$$

This equation permits calculation of capillary conductivity coefficients at any specified tension within the range of measurement if the water flux (v) through the cylinder and the gradient of the logarithm of tension are known. Water flux is measured by means of bubble tubes and is constant at all tensions throughout the cylinder at steady state. The logarithm tension gradient is measured by graphically determining the slope of the curve fitted to the distribution of tension plotted on semi-log paper at the tension for which the conductivity is to be calculated.

The above procedure was used to determine values of λ in all four cylinders at all four temperatures over a range of tensions.

Since soil moisture content could not be determined in the soil cylinders with the equipment available, it was necessary to determine moisture content at various tensions and at the four temperatures on separate soil samples. This was done in small lucite cylinders, 34 mm inside diameter and 100 mm deep, which had a tensiometer cup of the same type used in the large cylinders running the length of the central axis (Figure 5). These cylinders have a capacity of about 100 cc of soil.
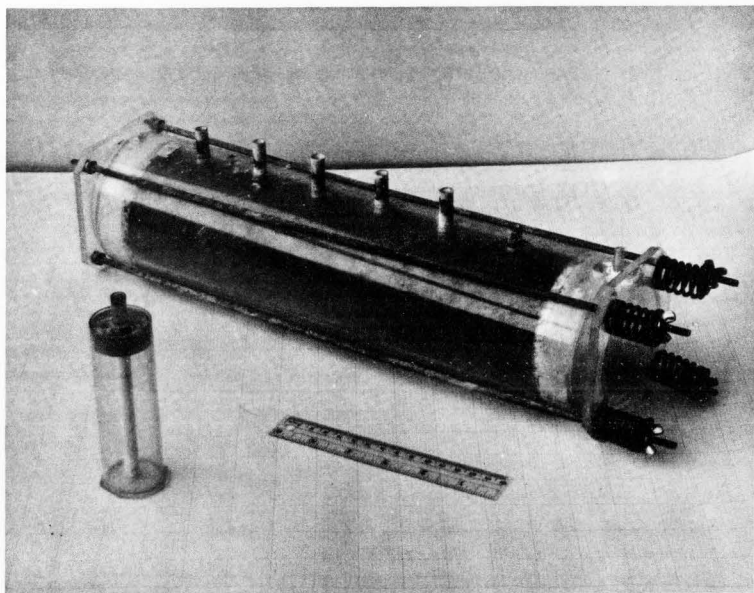
Figure 5. Soil moisture release cylinder without soil (lower left) and soil moisture conductivity cylinder filled with soil.

Three of these cylinders, one for each soil, were filled with a weighed amount of air-dry soil to the approximate bulk density of the same soil in the large cylinders. The soil was allowed to saturate slowly by adding water through the tensiometer cups. The cylinders were placed in the air bath and a constant low tension applied to the water within the tensiometer cups. After about a week the cylinders were removed and weighed, then returned to the air bath and subjected to a slightly greater tension. This procedure was repeated many times at different temperatures but always under conditions of decreasing moisture content (drying). When a lesser tension was desired, the cylinder was first saturated and then brought to the desired tension.

All weight changes were attributed to changes in soil moisture content. The oven-dry equivalent weight of the soil and the weight of each cylinder with its tensiometer cup filled with water were used in conjunction with moist weights to calculate moisture content by weight of each soil over a range of tensions at the four temperatures.

The results of these calculations were quite erratic. There was a tendency for moisture content at a given tension to increase with increasing temperature, especially when the soils were held at the higher temperatures for a month or more. This indicated that temperature changes were affecting something in addition to soil-water energy relations, perhaps a biotic factor.

In an attempt to avoid prolonged exposure of the soil to a single temperature, the cylinders containing the subalpine soil and the Millville soil were placed in a water bath and the cylinders were weighed after one day exposure to any fixed tension and temperature. The cylinder containing the mountain brush zone soil was treated somewhat differently. Its

moisture content was held constant at several values in succession and
its tension at various temperatures was read on a small bore manometer.
The soil was not held at any temperature other than room temperature
(20°C) for more than one day. The data so obtained were less erratic
and were amenable to multiple regression analysis which was utilized to
obtain equations of soil moisture tension as a function of temperature
and soil moisture content. The least squares approach of multiple
regression analysis was deemed more accurate than attempting to fit
curves to the data by eye.

RESULTS

The conductivity data were collected during three separate periods,
the main differences between periods being the tension of water at the
inlet side of the soil moisture conductivity cylinders. During period I
(March 23 to April 20, 1962), the water at the inlet side was at atmos-
pheric pressure (zero tension). During period II (May 3 to July 28, 1962)
the tension in the inlet chamber was about 150 centimeters of water
equivalent suction, and during period III (November 15, 1962, to February
28, 1963) inlet tension was about 50 centimeters of water. During all
three periods the tension on the outlet chamber was equivalent to about
700 centimeters of water.

The basic data consisting of tension distributions, flow rates, and
moisture content data, are tabulated by dates in Appendix I. Cylinder A
contained the subalpine clay loam at a bulk density of 1.075. Cylinder
B contained subalpine clay loam at a bulk density of 1.133. Cylinder C
contained the mountain brush zone soil at 1.060, and Cylinder D contained
Millville silt loam at 1.305. All calculations in subsequent sections
are based on these data.

Due to leaks and various other equipment failures, the amount of
data collected varies from cylinder to cylinder. The two cylinders
containing the subalpine soil operated satisfactorily during period I
but developed leaks during period II resulting in scanty data for this
period. During period III these two cylinders again operated satisfac-
torily with only an occasional leak. The cylinder containing the brush
zone soil developed numerous persistant leaks during the first two

periods so that only during period III is there sufficient data for analysis of temperature dependence. The cylinder containing the Millville silt loam functioned properly during all three periods and yielded the most complete set of data.

Conductivity as a function of temperature and moisture tension

Representative calculations of soil moisture conductivity coefficients as functions of temperature and tension are presented in Appendix II. In brief, the procedure consists of plotting soil moisture tension distribution and graphically determining the tension gradient $(\frac{d\tau}{dx})$ at several selected moisture tension values. The conductivity coefficient is the average measured flux divided by the tension gradient.

Soil moisture tension gradient values derived from the tensiometer data are tabulated by cylinder and date in Appendix II. The corresponding conductivity coefficients are also tabulated by dates in Appendix II.

Curves relating capillary conductivity to soil moisture tension at 12° and 40°C are presented on logarithmic scales in Figures 6 through 10. With the exception of Figure 9, all of these curves are based on data collected during period III because insufficient data were obtained during the first two periods to define satisfactory curves for any but the Millville soil. In all cases, 20° and 30°C curves generally lie between the 12° and 40°C curves but the differences between 12° and 20°C curves and between the 30° and 40°C curves are very small. The 20° and 30°C curves were not plotted because most of them lie so close to the plotted 12° and 40°C curves that confusion would result if they were plotted on the same graph.
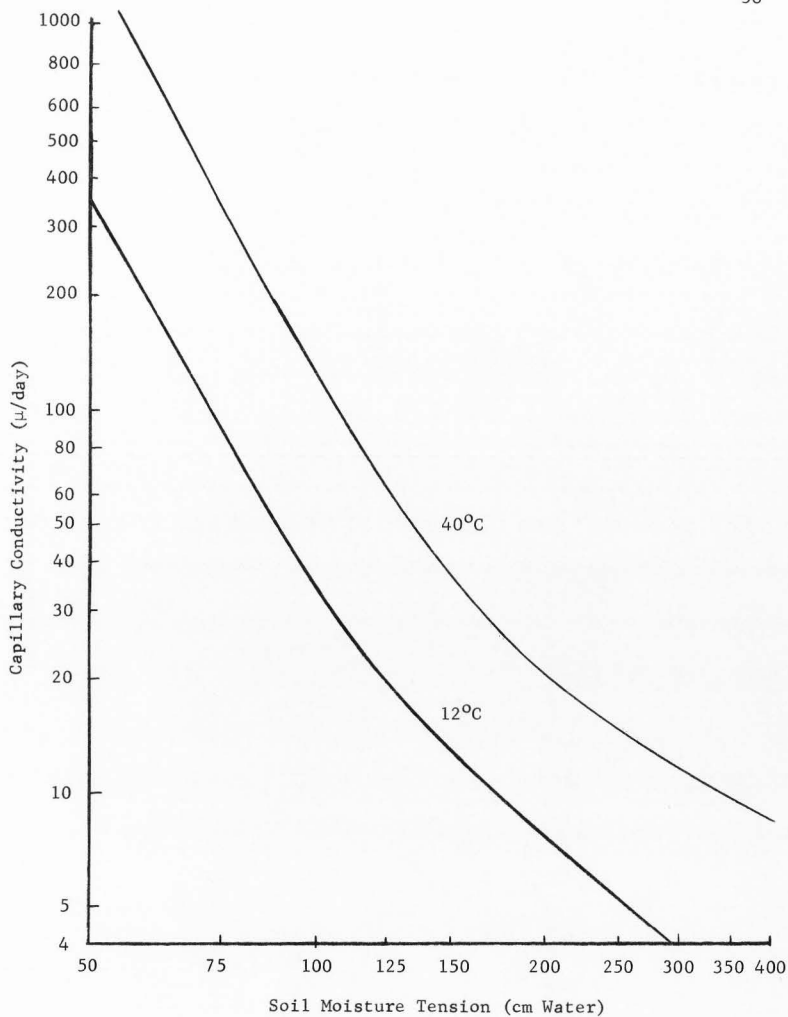
Figure 6. Capillary conductivity in cylinder A (subalpine clay loam) at 12° and 40°C as a function of soil moisture tension during period III
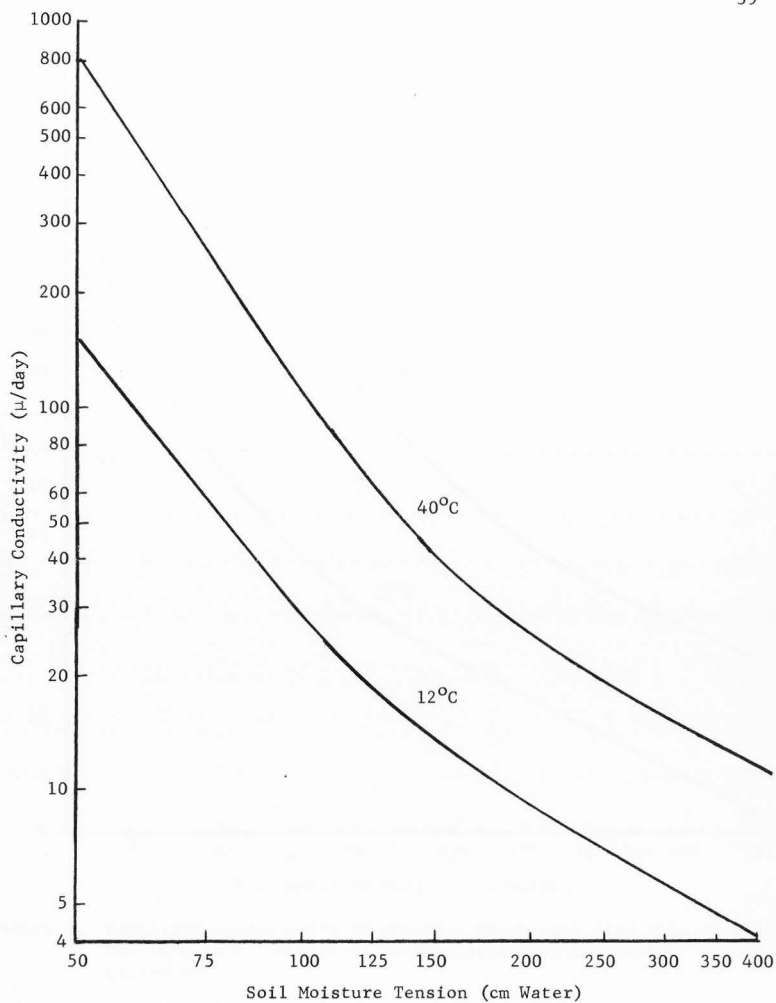
Figure 7. Capillary conductivity in cylinder B (subalpine clay loam) at 12° and 40°C as function of soil moisture tension during period III
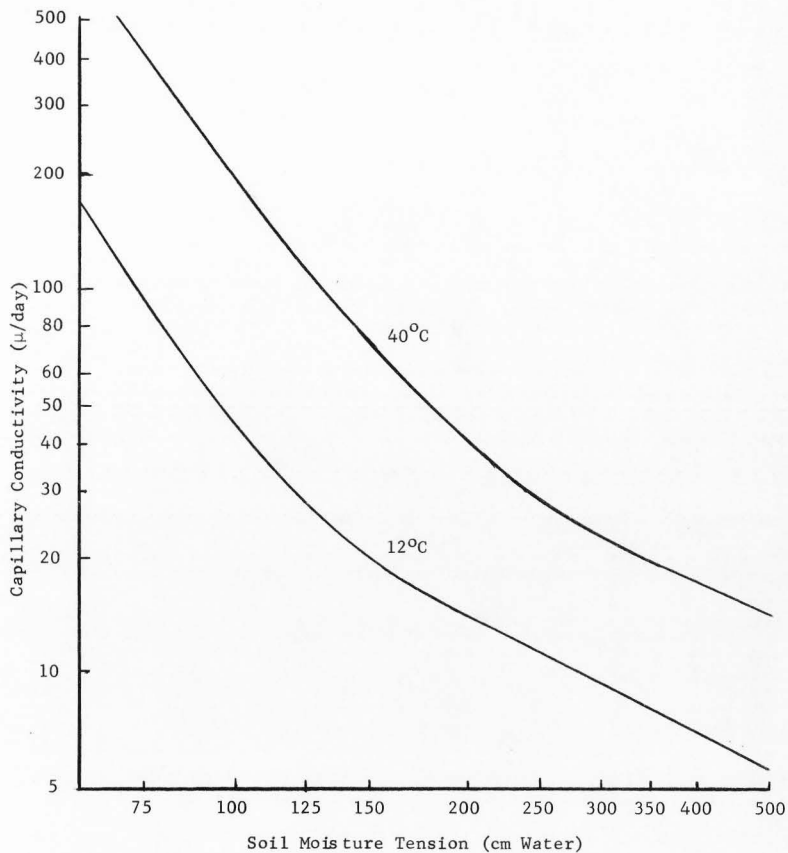
Figure 8.   Capillary conductivity of mountain brush zone clay loam at 12°
and 40°C as a function of soil moisture tension during
period III
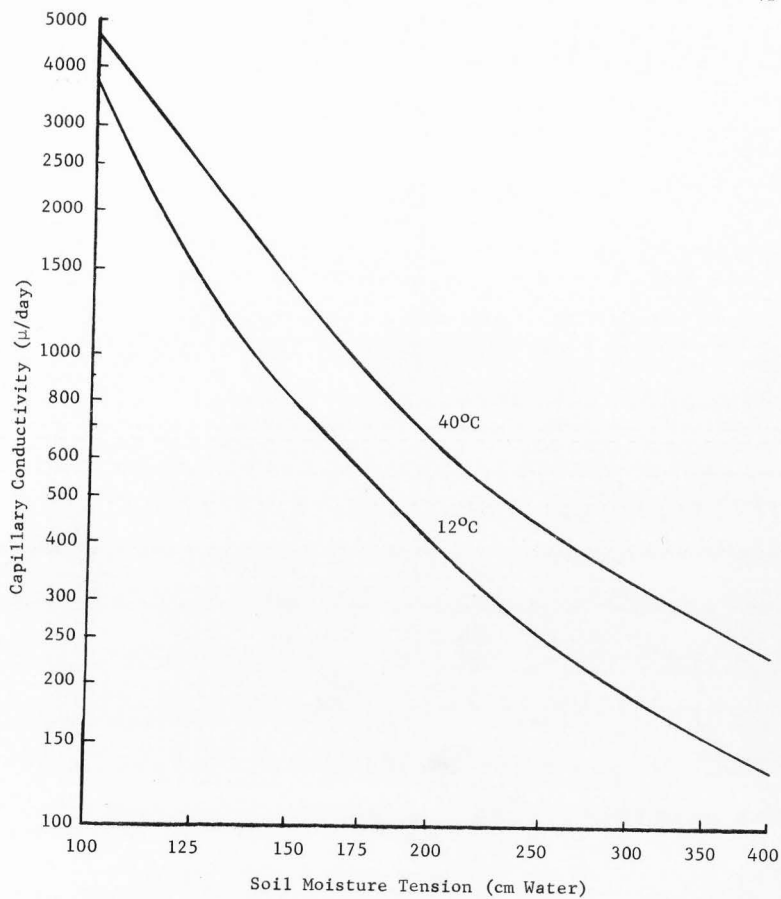
Figure 9.   Capillary conductivity of Millville silt loam at 12° and 40°C
as a function of soil moisture tension during period I
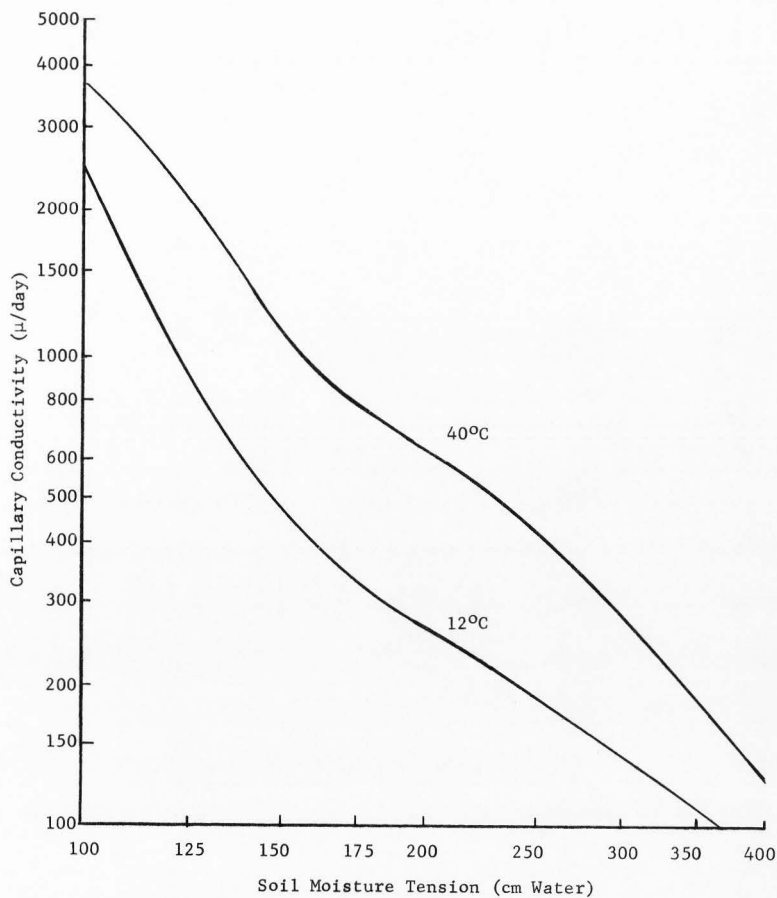
Figure 10. Capillary conductivity of Millville silt loam at 12° and 40°C as a function of soil moisture tension during Period III

Figures 6 and 7 show that conductivities in the two cylinders containing subalpine soil are similar but the soil with the greater bulk density (cylinder B) had a lower conductivity at low tensions and a higher conductivity at high tensions that the more loosely packed soil (cylinder A).

According to Figure 8, the conductivity characteristics of the mountain brush zone clay loam are similar to those of the subalpine soil. Conductivity coefficients are somewhat higher but temperature effects appear essentially the same.

Capillary conductivity coefficients of Millville silt loam during periods I and III are shown in Figures 9 and 10. These coefficients are much higher than those of the mountain soils. Comparison of the two figures shows the decline in conductivity with time that apparently occurred in all four cylinders.

Soil moisture tension as a function of temperature and moisture content

The basic data on moisture retention of the three soils at various temperatures are tabulated in Appendix I. These data are too variable for accurate free-hand curve fitting so it was necessary to resort to multiple regression techniques to derive moisture release curves for each of the three soils at each of the four temperatures. An equation relating tension to moisture content and temperature was calculated on the University IBM 1620 for each soil. A good fit was obtained in all three cases; the R^2 was 0.974 for the subalpine soil equation, 0.980 for the brush soil, and 0.985 for Millville silt loam. The equations are given in Appendix III. Values of soil moisture tension calculated from these equations are listed in Table 17 in Appendix III.

Soil moisture conductivity as a function of
temperature and moisture content

Since moisture content distribution in the conductivity cylinders
was not measured directly, the procedure used in this study yields mois-
ture conductivity coefficients that are functions of moisture tension
rather than of moisture content. If we wish to know the conductivity
at a particular moisture content and temperature, we must know the soil
moisture tension at that moisture content and temperature; then we can
determine conductivity from the tension-conductivity relation. The
computed soil moisture tension values given in Table 17 at various mois-
ture contents and temperatures were used to convert the conductivity
coefficients from functions of tension to functions of moisture content.
The results are tabulated in Appendix IV, along with a description of
methods used to calculate them. Conductivity coefficients calculated
from data obtained during period III are presented graphically in
Figures 11 through 14.

Because of the inverse relation between tension and temperature at
fixed moisture content (see Table 17) and the inverse relation between
conductivity and tension, the temperature dependence of conductivity at
fixed moisture content is greater than the temperature dependence of
conductivity at fixed tension. At a given moisture tension, conductivity
increases as temperature increases; and at a given moisture content,
tension decreases as temperature increases, resulting in an increase in
conductivity over and above that which would occur if tension remained
constant. One consequence of this is that when conductivity is plotted
as a function of moisture content the curves for the four temperatures
are distinct from one another whereas the curves relating conductivity
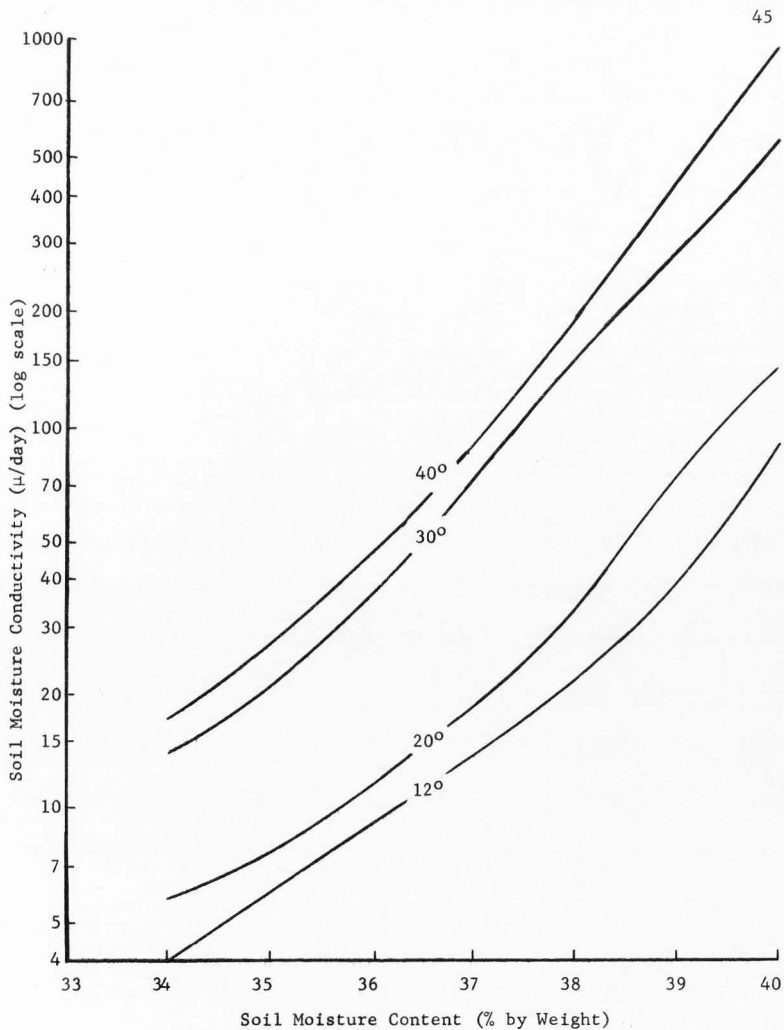
Figure 11. Soil moisture conductivity at 12°, 20°, 30°, and 40°C over a range of moisture contents: Cylinder A, period III
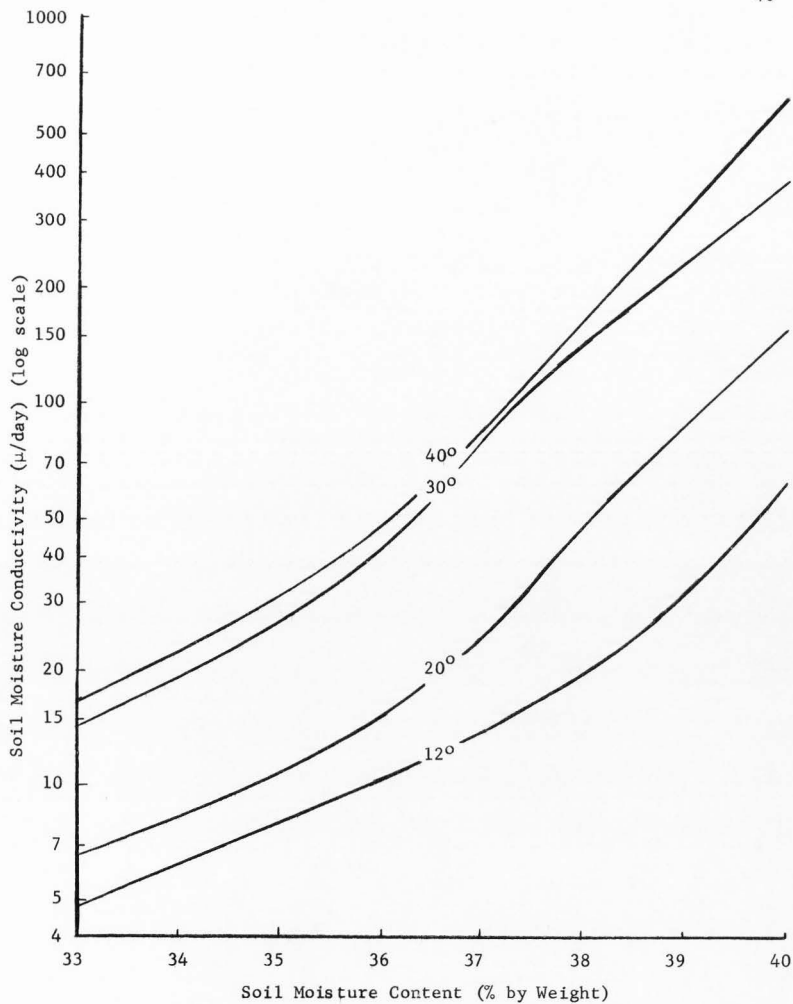
Figure 12.   Soil moisture conductivity at 12°, 20°, 30°, and 40°C over a
range of moisture contents: Cylinder B, period III
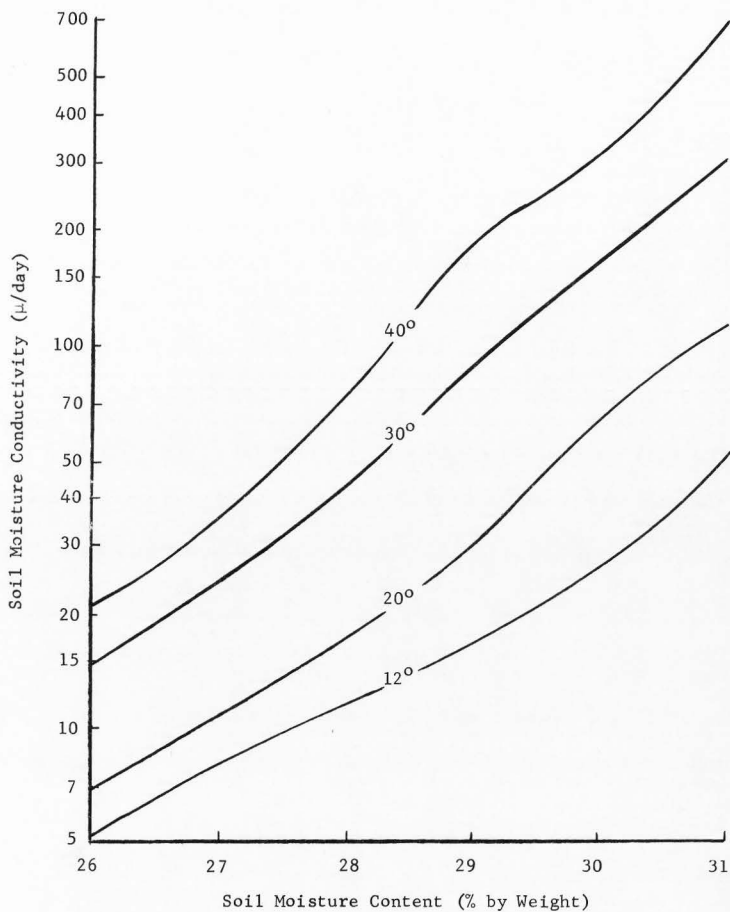
Figure 13. Soil moisture conductivity at 12°, 20°, 30°, and 40°C over a range of moisture contents: Cylinder C, period III
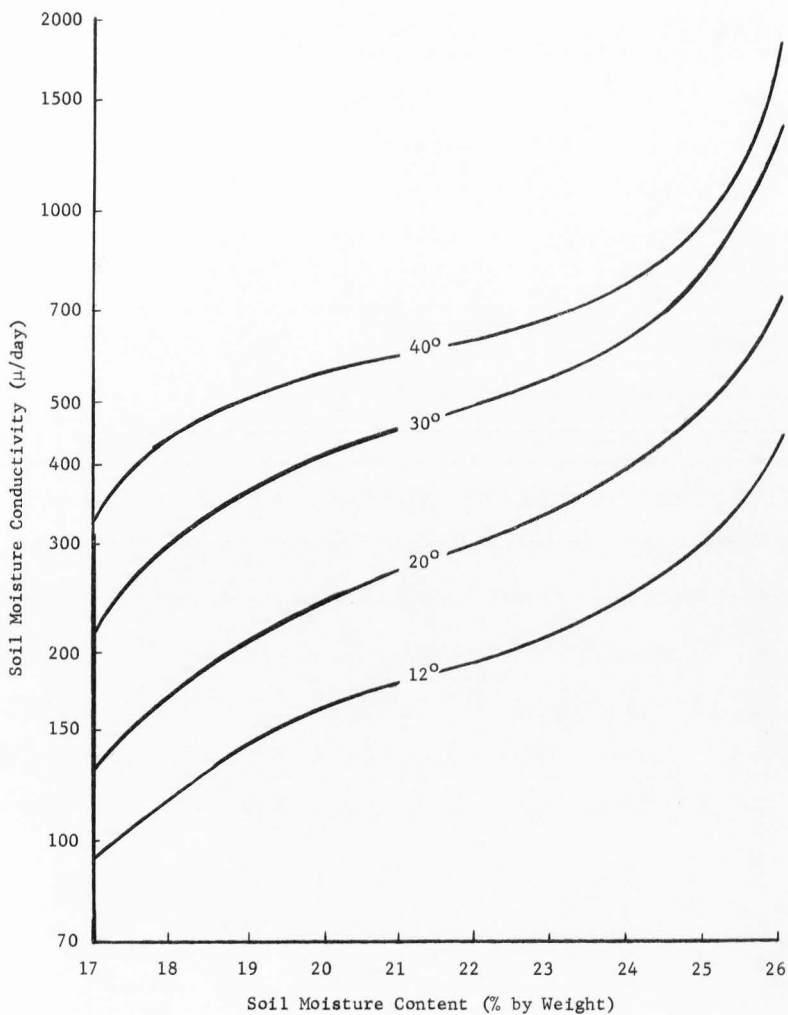
Figure 14. Soil moisture conductivity at 12°, 20°, 30°, and 40°C over a range of moisture contents

and tension are close together at 12° and 20°C and tend to overlap at 30° and 40°C.

Activation energy

Values of the coefficient b in the equation

$$b = - \frac{d \ln \lambda}{d(T^{-3})} \qquad (30)$$

were calculated for all of the sets of moisture conductivity data given in Appendix IV using the linear regression methods described in Appendix V. In general there were no significant relations between b and moisture content or period of measurement. Nor was there a significant difference in b between the two cylinders containing the subalpine clay loam.

The average b coefficients for each soil are as follows:

```
subalpine clay loam  . . . . . (18.25 ± 1.39) x 10⁷
mountain brush clay loam . . . (21.53 ± 2.27) x 10⁷
Millville silt loam  . . . . . (11.17 ± 0.57) x 10⁷
```

These averages are based on all conductivity values in Appendix IV and the limits are 95 percent confidence limits based on pooled deviations from average regression. All three coefficients are significantly greater than 5.93×10^7, the b values for viscosity of free water.

The corresponding activation energies at 20°C are:

```
subalpine clay loam  . . . . . 12.66 ± 0.97 Kilocalories per mole
mountain brush clay loam . . . 14.93 ± 1.58      "         "    "
Millville silt loam  . . . . .  7.75 ± 0.40      "         "    "
free water viscosity . . . . .  4.11             "         "    "
```

DISCUSSION

The activation energies for soil moisture movement under the experi-
mental conditions range from nearly 2 to more than 3 times as great as
that of free water viscosity. This means, among other things, that the
temperature dependence of moisture mobility in the range of moisture
contents studied is greater than equation (27),

$$\lambda = k \frac{\rho g}{\eta} , \tag{27}$$

would predict if η is taken as viscosity of normal free water.
This result is in agreement with Rosenqvist (1959) and Kunze and Kirkham
(1961) whose studies suggest increased viscosity of soil water.

In order to compare the steady state data obtained here with results
of transient state studies we must be certain that the correct rate
coefficients are used to calculate activation energy. Ideally, the rate
coefficients used for this purpose would be dependent upon temperature
alone and all other sources of variation would be fixed or eliminated.
In the case of steady state moisture movement, the rate coefficients
would be the proportionality factors between flow rate and driving force.
All properties of the system other than mobility of the water itself
should remain constant; the solid phase and the moisture content should
remain the same at all temperatures.

In this study there may have been changes in the solid phase of the
soil and certainly there was some variation in the moisture contents at
which conductivity coefficients were calculated. These sources of

variation are inherent in a study of this type but have been minimized as much as practicable.

The transient flow case is more difficult in some ways than the steady state flow case used here. It is not always clear which are the correct rate constants. The diffusivity coefficient D as defined in equation (8) is apparently a satisfactory rate coefficient, being a proportionality factor between flow rate and concentration gradient. The sorptivity coefficient S of equation (14) and the coefficient a of equation (15) are not true rate coefficients because there are varying driving forces incorporated within them. However, the activation energy of soil moisture mobility can be derived from sorptivity coefficients. If we combine equations (5) and (14),

$$q = A \left(\frac{\gamma \cos\theta}{\eta}\right)^{\frac{1}{2}} t^{\frac{1}{2}} \tag{5}$$

$$q = S t^{\frac{1}{2}} \quad , \tag{14}$$

we obtain

$$S^2 = A^2 \cos\theta \frac{\gamma}{\eta} \tag{33}$$

Converting equation (33) to natural logarithms and differentiating with respect to $\left(\frac{1}{T}\right)$

$$2 \frac{d \ln S}{d\left(\frac{1}{T}\right)} = \frac{d \ln \gamma}{d\left(\frac{1}{T}\right)} - \frac{d \ln \eta}{d\left(\frac{1}{T}\right)} \quad , \tag{34}$$

A and θ are assumed to be independent of temperature. If all terms are multiplied by R, this may be written:

$$E_S = E_\gamma - E_\eta \tag{35}$$

in which E_S is $2R \dfrac{d \ln S}{d(\frac{1}{T})}$, E_γ is $R \dfrac{d \ln \gamma}{d(\frac{1}{T})}$, and E_η is $R \dfrac{d \ln \eta}{d(\frac{1}{T})}$. Free

water at 25°C has an E_γ of -0.38 kilocalories per mole and an E_η of 4.00

kilocalories per mole; thus E_S would be 3.62 kilocalories per mole if γ

and η of soil water were the same as those of free water. The average of

the values of $R \dfrac{d \ln S}{d(\frac{1}{T})}$ determined by Biggar and Taylor (1960) is 2.07

kilocalories per mole at an average temperature of 25°C, giving an E_S of

4.14 for soil water during sorption. This suggests that $(E_\gamma - E_\eta)$ of

soil water during sorption is greater than $(E_\gamma - E_\eta)$ of free water.

In my steady state study activation energy averaged 7.75 kilocalories

per mole in Millville silt loam, the same soil Biggar and Taylor used.

There are at least two reasons why the E_a of my study should be larger

than the E_S of Biggar's study. E_a in my study is assumed to be the

result of temperature dependence of water viscosity and density alone

and is therefore equivalent to $(-E_\eta)$, water density normally being only

slightly temperature dependent. This means that, under identical condi-

tions, E_a and E_S differ by an amount equal to E_γ. Since E_γ is a negative

quantity, equation (35) indicates that E_a or $-E_\eta)$ should be greater than

E_S.

The moisture content at which flow is occurring should also be

considered. According to Colman and Bodman (1944) the bulk of liquid

flow during infiltration occurs at moisture tensions of about 20 cm

water suction. Thus, most of the liquid flow in Biggar's infiltration

study probably took place at relatively low soil moisture tensions

compared to the 100 to 400 cm of water tension range covered in my study.

Although no significant relation between E_a and moisture content or

tension was found in that range, it is reasonable to expect E_a of soil

water to approach E_a of free water as moisture content approaches

saturation and, therefore, at the higher moisture contents at which most of the liquid flow occurred in Biggar's study, a smaller E_a would be expected.

In evaporation studies with Millville silt loam, Wiegand and Taylor (1960) found $R \dfrac{d \ln a}{d(\frac{1}{T})}$ averaged 6.9 kilocalories per mole, a being the coefficient in the equation

$$Q = at^{0.92} \qquad (15)$$

in which Q is cumulative evaporation from a soil column with a water table at the bottom. As stated earlier, "a" is not a true rate coefficient because it contains a varying driving force component. Because of this, it is not possible to make a concise comparison between apparent activation energy calculated by Wiegand and Taylor and that obtained for the same soil in my study. It is interesting to note, however, that the value of E_a obtained in my study (7.75 kilocalories per mole) falls within the range of values of activation energy calculated by Wiegand and Taylor (6.9 $\pm$ 2.3 kilocalories per mole).

The reports of Stewart (1962), Jackson (1963) and Anderson et al. (1963) indicate that the temperature dependence of liquid movement during infiltration of water into soil is equal to or slightly greater than the temperature dependence of free water viscosity. This does not necessarily mean that the fluid properties of water flowing through soil are the same as those of free water. If equations (7) and (27) are combined we obtain the following definition of the diffusivity coefficient:

$$D = \frac{k\rho g}{\eta} \frac{\partial \psi}{\partial \theta} \qquad (36)$$

In addition to viscosity and density, diffusivity coefficients also contain another temperature sensitive component $(\frac{\partial \psi}{\partial \theta})$ which, according to Stewart (1962) tends to decrease as temperature increases and thereby partially compensates for the effect of temperature on viscosity. In both Stewart's and Jackson's studies any changes in temperature dependence of viscosity were essentially cancelled out by changes in $\frac{\partial \psi}{\partial \theta}$. Anderson et al. obtained apparent activation energy values greater than that of free water viscosity. Although they attributed the activation energy in excess of that of free water viscosity to the energy required to extend air-water interfaces, it is equally probable that it is a result of greater viscosity of soil water.

CONCLUSIONS

Theoretical considerations suggest that viscosity of water near soil-water interfaces is greater than that of free water. Measurements of self-diffusion of water in unsaturated soil systems tend to confirm this hypothesis. Although presently developed theory is not adequate to provide means of actually measuring soil water viscosity, the activation energy concept can be used to demonstrate the existence of viscosity variations.

Results of this approach reported herein indicate that the increased viscosity adjacent to soil-water interfaces materially influences flow rate at soil moisture tensions as low as 100 cm of water. Apparent activation energies for soil moisture movement in Millville silt loam were nearly twice that of free water viscosity and more than 3 times greater than free water fiscosity in the two clay loams. These results are indicative of several-fold increase in effective viscosity in the water conducting films.

According to available evidence, a simple correction based on the temperature dependence of free water viscosity will usually account for temperature-induced changes in soil moisture diffusivity at the low moisture tensions at which the bulk of liquid flow occurs during infil- tration. However, at greater tensions such as exist at field capacity, soil moisture conductivity appears to be much more temperature dependent than is free water fiscosity. The influence of temperature on moisture conductivity in this moisture range cannot be satisfactorily accounted for by a simple viscosity correction. No reliable alternative can be

suggested at this time; further study is required to develop accurate correction factors for any soils other than the ones tested in this experiment. The results of this experiment emphasize the need for careful temperature regulation in studies involving liquid movement in soils in the field moisture content range.

LITERATURE CITED

Anderson, D. M., A. Linville, and G. Sposito. 1963. Temperature fluctuations at a wetting front: III. Apparent activation energies for water movement in the liquid and vapor phases. Soil Sci. Soc. Am. Proc. 27: 610-613.

Biggar, J. W. 1956. On the kinetics of moisture flow in unsaturated soils. Unpublished Ph.D. dissertation, Utah State University Library, Logan.

Biggar, J. W. and S. A. Taylor. 1960. Some aspects of the kinetics of moisture flow into unsaturated soils. Soil Sci. Soc. Am. Proc. 24: 81-85.

Bouyoucos, G. J. 1915. Effect of temperature on some of the most important physical processes in soils. Mich. Agr. Exp. Sta. Tech. Bul. 22. 63 p.

Briggs, L. J. 1897. The mechanics of soil moisture, U. S. Dept. Agr. Bur. Soils Bul. 10. 24 p.

Buckingham, E. 1907. Studies on the movement of soil moisture. U. S. Dept. Agr. Bur. Soils Bul. 38. 61 p.

Carman, P. C. 1939. Permeability of saturated sands, soils and clays. J. Agr. Sci. 29: 262-273.

Childs, E. C. and N. Collis-George. 1948. Soil geometry and soil water equilibrium. Disc. Faraday Soc. 3: 78-85.

Childs, E. C. and N. Collis-George. 1950. The permeability of porous materials. Proc. Roy. Soc. (London) 201(Series A): 392-405.

Colman, E. A. and G. B. Bodman. 1944. Moisture and energy conditions during downward entry of water into moist and layered soils. Soil Sci. Soc. Am. Proc. 9: 3-11.

Dorsey, N. E. 1940. Properties of ordinary water-substance. Reinhold Publishing Corp., New York. p. 183, 514-515.

Gardner, W. 1919. Movement of moisture in soil by capillarity. Soil Sci. 7: 313-317.

Gardner, W. R. 1959. Diffusivity of soil water during sorption as affected by temperature. Soil Sci. Soc. Am. Proc. 23: 406-407.

Glasstone, S., K. J. Laidler, and H. Eyring. 1941. The theory of rate processes. McGraw-Hill Book Co., New York. p. 477-484.

Grunberg, L. and A. H. Nissen. 1949. The energies of vaporization, viscosity, and the structure of liquids. Faraday Soc. Trans. 45: 125-137.

Innes, K. K. 1956. Temperature dependence of viscosity of liquids. J. Phys. Chem. 60: 817-818.

Jackson, R. D. 1963. Temperature and soil-water diffusivity relations. Soil Sci. Soc. Am. Proc. 27: 363-366.

King, F. H. 1892. Observations and experiments on the fluctuations in the level and rate of movement of groundwater on the experiment station farm and at Whitewater, Wis. Ninth Ann. Rpt. Wis. Agr. Expt. Sta. p. 129-218.

Klute, A. 1952. A numerical method for solving the flow equation for water in unsaturated materials. Soil Sci. 73: 105-116.

Kunze, R. J. and D. Kirkham. 1961. Deuterium and the self-diffusion coefficient of soil water. Soil Sci. Soc. Am. Proc. 25: 9-12.

Litowitz, T. A. 1952. Temperature dependence of the viscosity of associated liquids. J. Chem. Phys. 20: 1088-1089.

Low, P. F. 1960. Viscosity of water in clay systems. Eighth National Conference on Clays and Clay Minerals Proc. p. 170-182.

Moore, R. E. 1939. Water conduction from shallow water tables. Hilgardia 12: 383-426.

Moore, R. E. 1940. The relation of soil temperature to soil moisture: pressure potential, retention, and infiltration rate. Soil Sci. Soc. Am. Proc. 5: 61-64.

Phillip, J. R. 1957. The theory of infiltration: 4 sorptivity and algebraic infiltration equations. Soil Sci. 84: 257-264.

Richards, L. A. 1952. Report of the Subcommittee on Permeability and Infiltration, Committee on Terminology, Soil Science Society of America. Soil Sci. Soc. Am. Proc. 16: 85-88.

Rosenqvist, I Th. 1959. Physico-chemical properties of soils: soil water systems. J. Soil Mechanics and Foundations Div. Am. Soc. Civil Eng. 85(SM2): 31-53.

Stewart, G. L. 1962. Water content measurement by neutron attenuation and applications to unsaturated flow of water in soil. Unpublished Ph.D. dissertation, Washington State University Library, Pullman.

Swartzendruber, D., M. F. de Boodt, and D. Kirkham. 1954. Capillary intake rate of water and soil structure. Soil Sci. Soc. Am. Proc. 18: 1-7.

Taylor, S. A. and G. L. Stewart. 1960. Some thermodynamic properties of soil water. Soil Sci. Soc. Am. Proc. 24: 243-247.

Wang, J. H., C. V. Robinson, and I. S. Edelman. 1953. Self-diffusion and structure of water. III. J. Am. Chem. Soc. 75: 466-477.

Washburn, E. W. 1921. Dynamics of capillary flow. Phys. Rev. 17: 273-283.

Wiegand, C. L. and S. A. Taylor. 1960. The temperature dependence of the drying of soil columns. Proc. 7th International Congress of Soil Science, Madison, Wis. 1: 169-178.

Wu, T. H. 1964. A nuclear magnetic resonance study of water in clay. J. Geophys. Res. 69: 1083-1091.

APPENDIXES

Appendix I. Basic data

Table 2. Average flow rates and soil moisture tension distributions in
cylinder A by dates

Date	Temp.	v	Soil moisture tension at points					
			1	2	3	4	5	6
	°C	mm/day	- - - - - - centimeters water - - - - - - -					
3/23/62	40	4.94	22.3	27.4	29.2	31.6	39.8	61.3
3/24	40	4.82	25.4	29.2	30.9	32.6	41.2	62.3
3/29	30	3.61	24.5	28.3	31.7	32.8	40.7	60.4
4/2	30	3.62	23.1	27.6	30.0	32.4	41.0	55.3
4/6	20	2.79	20.1	24.5	27.0	28.0	37.3	52.9
4/11	20	2.95	20.4	25.2	27.3	29.0	37.3	51.9
4/20	12	2.57	22.8	25.9	29.7	30.7	39.7	59.3
5/3	40	0.325	112	121	131	147	192	324
5/22	30	0.134	144	153	166	188	238	347
5/25	30	0.154	146	155	168	192	242	353
7/1	20	0.146	136	151	172	202	260	386
7/28	12	0.232	140	159	186	219	277	384
11/15	12	0.333	42.2	44.4	51.1	61.6	86.0	192
11/20	12	0.379	46.0	50.5	58.2	66.9	90.8	192
11/22	12	0.267	53.9	58.0	65.6	75.5	102	207
11/29	12	0.305	54.9	58.5	67.5	78.0	104	212
12/11	20	0.293	35.4	39.0	43.1	55.7	74.0	179
12/14	20	0.541	35.8	43.6	50.5	59.5	78.7	181
12/27	20	0.206	59.7	64.7	69.0	81.9	107	216
12/29	20	0.191	63.4	66.3	74.1	83.6	110	220
1/3/63	20	0.672	50.8	58.6	67.4	80.3	106	221
1/18	30	0.926	53.0	60.0	67.1	80.3	104	213
1/22	30	0.970	48.0	55.0	63.3	77.6	103	214
1/25	30	0.841	49.2	52.1	60.0	71.4	92.7	192
1/31	40	1.11	52.8	57.7	66.0	79.1	106	221
2/12	40	0.772	56.4	60.5	69.6	82.6	125	489
2/15	40	0.801	65.2	67.8	80.4	93.6	143	472

Table 3. Average flow rates and soil moisture tension distributions in cylinder B by dates

Date	Temp	v	Soil moisture tension at points					
			1	2	3	4	5	6
	^{o}C	mm/day	- - - - - - centimeters water - - - - - - -
3/23/62	40	4.90	29.2	32.3	35.9	44.8	55.6	93.9
3/24	40	4.64	29.2	32.3	35.6	41.7	54.9	93.2
3/29	30	3.56	27.6	31.4	33.3	40.6	51.2	85.6
4/2	30	3.68	27.9	30.3	32.3	38.2	47.4	77.3
4/6	20	2.69	25.2	27.0	30.6	34.5	44.2	75.9
4/11	20	2.84	22.5	27.6	30.1	34.1	44.2	74.2
4/20	12	2.04	23.9	26.6	32.7	34.8	45.5	78.0
5/22	30	0.146	169	196	228	268	338	461
2/25	30	0.105	178	203	234	273	344	465
7/1	20	0.142	146	176	212	269	361	507
7/28	12	0.107	152	184	228	282	375	600
11/15	12	0.272	42.2	50.0	66.4	95.2	178	373
11/20	12	0.223	50.1	60.6	73.5	102	189	392
11/22	12	0.274	47.6	58.5	65.9	106	192	395
11/29	12	0.326	46.1	53.9	70.7	94.0	170	365
12/11	20	0.447	48.1	55.6	69.2	91.4	153	356
12/14	20	0.385	43.8	51.5	66.5	87.9	150	350
12/27	20	0.251	61.7	69.3	83.2	105	154	324
12/29	20	0.262	66.0	71.6	85.5	105	154	322
1/3/63	20	0.486	51.1	59.0	74.1	97.5	147	326
1/18	30	0.798	55.3	61.5	77.7	97.5	144	316
1/22	30	0.940	51.2	59.0	75.5	95.9	148	339
1/25	30	0.800	50.0	55.6	68.0	91.8	125	303
1/31	40	1.005	50.8	57.2	69.0	83.8	135	351.
2/15	40	0.716	53.1	56.8	71.3	95.3	156	435

Table 4. Average flow rates and soil moisture tension distributions in cylinder C

Date	Temp.	v	Soil moisture tension at points					
			1	2	3	4	5	6
	°C	mm/day	- - - - - - centimeters water - - - - - -					
3/23/62	40	5.36	29.5	29.8	34.5	40.6	56.4	112
3/24	40	5.20	29.5	29.8	35.2	40.6	56.8	114
3/29	30	3.83	28.3	30.7	33.8	38.9	56.1	120
4/2	30	3.81	28.3	28.4	31.8	35.5	51.3	112
4/6	20	2.93	24.2	24.3	27.7	31.7	47.2	105
4/20	12	2.30	26.6	28.0	32.2	35.5	53.4	116
5/3	40	1.25	104	124	145	177	273	474
5/22	30	0.303	155	171	195	227	316	458
5/25	30	0.240	166	183	207	238	323	457
11/15	12	0.316	53.0	63.8	83.8	121	223	411
11/20	12	0.307	62.3	73.4	93.1	129	232	430
11/22	12	0.359	59.1	76.6	95.9	134	239	430
11/29	12	0.398	55.0	70.6	84.8	122	220	409
12/11	20	0.431	54.0	63.9	74.3	111	199	398
12/14	20	0.499	54.0	65.5	79.0	109	191	369
12/27	20	0.348	76.8	87.3	105	135	215	403
12/29	20	0.412	74.6	84.1	103	131	212	382
1/3/63	20	0.626	66.1	77.4	96.9	127	211	405
1/18	30	0.820	69.3	78.7	96.9	128	212	399
1/22	30	0.882	65.5	78.3	98.4	129	213	406
1/25	30	0.768	65.5	75.4	92.1	119	199	390
1/31	40	0.891	64.6	73.2	93.0	125	221	409
2/15	40	1.32	63.6	71.2	88.2	117	221	515

Table 5. Average flow rates and soil moisture tension distributions in
cylinder D

Date	Temp.	v	Soil moisture tension at points					
			1	2	3	4	5	6
	°C	mm/day	- - - - - - centimeters water - - - - - - -					
3/23/62	40	14.04	81.4	90.0	97.7	126	169	297
3/24	40	14.38	81.4	90.0	97.7	126	169	298
3/29	30	11.11	81.9	89.1	97.8	125	164	291
4/2	30	11.27	81.9	89.1	98.1	122	159	277
4/6	20	9.12	81.3	88.2	95.5	121	158	285
4/11	20	8.71	82.7	89.6	96.8	122	160	286
4/20	12	7.67	92.4	98.9	111	137	182	318
5/3	40	5.31	152	162	181	223	296	491
5/22	30	3.21	172	185	205	247	320	462
5/25	30	3.26	171	185	206	248	321	452
7/1	20	2.21	155	172	199	248	333	501
7/8	20	1.55	200	221	252	308	401	512
7/13	12	2.38	157	179	199	250	307	463
7/28	12	2.16	160	175	200	245	324	341
11/15	12	3.94	97.8	112	136	188	271	440
11/20	12	3.48	107	120	144	195	278	449
11/22	12	3.78	105	120	143	200	283	454
11/29	12	3.81	96.6	111	135	187	302	440
12/11	20	4.67	91.1	104	126	178	260	445
12/14	20	4.78	87.9	101	123	175	257	442
12/29	20	4.80	115	132	156	201	269	435
1/3/63	20	5.57	106	123	146	192	258	426
1/18	30	6.84	104	119	141	182	248	412
1/22	30	7.02	100	116	137	179	247	412
1/25	30	6.58	104	118	139	182	247	412
2/12	40	6.82	109	122	142	182	242	378
2/13	40	6.69	116	129	152	192	253	385
2/15	40	6.89	111	125	146	186	245	375

Table 6. Moisture content of the subalpine clay loam at
various tensions and temperatures

Temp.	τ	P_w	Temp.	τ	P_w
°C	cm H_2O	%	°C	cm H_2O	%
12.0	36	43.3	40.0	98	37.3
20.0	26	43.1	20.0	205	35.3
30.0	34	42.8	12.0	207	35.7
40.0	24	43.0	41.0	199	33.9
12.0	37	43.3	12.0	208	35.6
20.0	36	42.9	20.0	208	34.6
31.0	35	42.2	30.0	317	33.4
20.0	35	42.2	40.0	274	33.1
40.8	34	42.4	12.0	333	33.0
12.0	70	41.0	20.1	363	32.9
30.0	44	41.6	40.0	243	32.8
40.0	43	41.6	20.0	345	32.6
20.0	83	38.6	30.0	341	32.0
30.0	79	38.6	12.0	341	33.2
40.0	93	37.7	19.5	340	32.0
12.0	100	39.5	30.0	340	31.6
30.0	97	38.8	41.5	338	30.2
40.0	97	37.2	12.0	431	31.2
12.0	103	38.6	19.7	434	30.7
30.5	102	38.0	30.4	425	30.4
12.0	137	37.7	40.4	404	29.6
20.0	162	35.6	20.1	693	30.8
30.0	205	34.1	40.1	668	30.7
40.0	161	35.4	12.0	695	30.4
20.0	104	37.9	30.0	665	30.8
12.0	106	37.9	40.0	754	29.8
20.0	101	37.5			

Table 7. Soil moisture tension of the mountain brush zone clay loam at various soil moisture contents and temperatures

P_w	Temp.	τ	P_w	Temp.	τ	P_w	Temp.	τ
%	°C	cm H_2O	%	°C	cm H_2O	%	°C	cm H_2O
28.5	18.3	183	26.9	14.3	340	25.9	13.7	555
28.5	31.5	164	26.9	25.7	292	25.9	27.5	516
28.5	20.2	179	26.9	25.4	290	25.9	35.1	425
28.5	31.3	158	26.9	31.1	246	25.9	40.4	379
28.5	40.5	130	26.9	31.2	237	25.9	13.4	546
28.5	20.0	181	26.9	39.4	199	25.9	29.4	496
28.5	20.0	178	26.9	40.8	181	25.9	29.7	479
28.5	21.0	168	26.9	41.0	172	25.9	40.5	385
28.5	31.2	146						
28.5	32.0	146	26.4	12.6	419	32.2	13.3	87
28.5	31.5	146	26.4	27.7	346	32.2	27.0	65
28.5	40.8	113	26.4	42.5	265	32.2	35.2	53
28.5	40.7	111	26.4	16.6	331	32.2	20.9	79
28.5	20.0	172	26.4	14.8	336	32.2	14.0	91
						32.2	38.8	53
27.5	18.5	271	26.2	13.8	275	32.2	28.6	664
27.5	18.5	268	26.2	25.4	454	32.2	39.5	501
27.5	18.6	266	26.2	31.9	420	32.2	12.5	867
27.5	31.0	221	26.2	42.5	325	32.2	26.6	677
27.5	40.1	179				32.2	39.5	474
27.5	20.0	241	25.6	14.5	645			
27.5	21.1	236	25.6	25.4	566	33.5	15.0	74
27.5	30.6	207	25.6	25.9	547	33.5	29.7	62
27.5	40.0	168				33.5	39.8	48
27.5	21.7	225	27.1	13.5	305	33.5	13.6	82
27.5	29.8	194	27.1	28.5	256	33.5	30.9	50
27.5	38.7	159	27.1	38.2	211	33.5	42.0	43
27.5	20.0	226	27.1	40.1	197	33.5	13.9	62
			27.1	29.7	232	33.5	28.3	45
27.0	20.0	285				33.5	38.9	38
27.0	30.1	244	36.0	12.5	49	33.5	14.2	73
27.0	30.0	245	36.0	26.6	34	33.5	27.0	43
27.0	41.9	189	36.0	39.5	34	33.5	35.2	31
27.0	42.1	189	36.0	14.1	50	33.5	20.9	60
						33.5	39.5	48

Table 8. Moisture content of Millville silt loam at
various tensions and temperatures

Temp.	τ	P_w	Temp	τ	P_w
^oC	cm H_2O	%	^oC	cm H_2O	%
12.0	70	36.2	41.0	199	29.7
20.3	66	35.5	12.0	208	30.5
12.0	98	36.6	20.0	208	29.7
20.0	93	35.8	20.0	345	22.2
30.5	92	35.6	30.0	341	21.7
40.0	92	34.9	12.0	341	22.1
30.0	32	35.8	19.5	340	22.3
20.0	34	36.2	30.0	340	21.5
12.0	34	36.4	41.5	338	21.0
12.0	106	36.1	12.0	431	21.5
20.0	101	35.7	19.7	434	21.0
40.0	98	35.3	30.4	425	19.6
12.0	103	35.9	40.4	428	19.4
40.0	97	35.0	20.1	693	18.6
30.5	102	35.1	30.0	317	22.0
20.0	205	31.0	30.0	665	18.5
12.0	207	30.6	40.0	342	21.8
30.0	205	29.9	40.1	668	18.1

Appendix II. Conductivity as a function of
temperature and soil moisture tension

Capillary conductivity coefficients as defined by Buckingham's
equation:

$$\lambda = \frac{v}{\left(\frac{\partial \psi}{\partial x}\right)} \qquad (3)$$

were calculated at several tensions for every set of data in Tables 2,
3, 4, and 5. These calculations consisted of the following three steps:

1) The moisture tension distribution on semi-log paper and a curve
was hand-fitted to the data. A separate curve was plotted for each set
of 6 tensiometer readings. The solid curve in Figure 4 is a good example
of a tension distribution curve. It was plotted from the actual data
obtained on 22 January 1963 for cylinder A (Table 2).

2) A number of fixed tensions were chosen for which conductivity
coefficients would be determined. The range of tension values selected
depended on the range of available data. The tension values chosen for
each cylinder are in the column headings of the tables in this appendix.
At each of these tensions the slope of the tension distribution curve
was measured graphically. This slope is equivalent to $\frac{d \log \tau}{dx}$ and was
multiplied by 2.303τ to convert it to tension gradient:

$$\frac{d\tau}{dx} = 2.303\tau \, \frac{d \log \tau}{dx} \qquad (31a)$$

The tension gradients so determined for each soil on each day of record
are presented in Tables 9, 10, 11, and 12.

3) Conductivity coefficients were then calculated by dividing the
average flux (macroscopic flow velocity) for the date of record by the
tension gradient at the tension of interest. This was done with each

tension gradient listed in Tables 1, 10, 11, and 12. The resulting coefficients are tabulated in Tables 13, 14, 15, and 16.

A representative calculation based on the solid curve in Figure 4 is as follows: at 100 cm water tension (2.0 on the logarithmic scale) the slope of the solid curve is 0.02753 cm^{-1} when corrected for differences in scale between the horizontal and vertical axes. The tension gradient at 100 cm is, then, 2.303 x 10 cm x 0.02753 - 6.34 cm H_2O/cm. According to Table 2 the average rate of moisture flow in cylinder A on 22 January 1963 was 0.970 mm per day. This flux divided by the gradient, 6.34, gives the conductivity coefficient: 0.153 mm per day, or 153μ/day as given in Table 13 for 100 cm tension on 22 January 1963. All conductivity coefficients in this appendix were calculated in this manner.

Table 9. Soil moisture tension gradients at several tensions by dates in cylinder A

Date	Temp. °C	Soil moisture tension (cm H2O)											
		30	50	75	100	125	150	175	200	250	300	350	400
		Soil moisture tension gradient cm H2O/cm											
2/23/62	40	0.462	3.70										
3/24	40	0.343	3.44										
3/29	30	0.555	3.44										
4/2	30	0.343	2.69										
4/6	20	0.718	3.20										
4/11	20	0.493	3.09										
4/20	12	0.587	3.38										
5/3	40				1.59	2.10	5.21	9.95	16.0	28.5	40.1	49.6	60.3
5/22	30						1.92	4.29	7.46	17.1	24.9	31.0	36.2
5/25	30						1.98	4.11	7.46	15.8	23.5	30.3	36.2
7/1	20					2.68	3.37	5.04	7.46	15.3	23.0	31.6	37.8
7/28	12					3.32	4.15	5.04	6.69	11.9	18.3	23.0	28.4
11/15	12		1.44	5.32	12.6	21.5	27.7	34.9	39.9	54.2			
11/20	12		1.02	4.27	10.9	18.8	27.7	34.9	39.9	48.8			
11/22	12		.704	2.90	7.98	11.8	17.1	30.1	37.0	41.6			
11/29	12			2.70	8.31	15.8	24.1	32.3	39.9	49.9			
12/11	20		2.00	6.23	16.1	29.6	39.2	45.7	58.2				
12/14	20		1.74	6.64	16.1	24.9	35.5	41.5	49.7				
12/27	20			2.24	6.83	13.6	22.6	32.3	39.9	54.2			
12/29	20			1.92	6.58	14.2	21.3	28.1	34.4	46.2			
1/3/63	20		1.33	2.80	6.58	14.2	24.1	32.3	47.4	65.3			
1/18	30		1.12	2.90	6.11	13.6	22.6	34.9	43.3	65.3			
1/22	30		1.38	3.45	6.34	13.6	25.8	41.5	58.2	93.8			
1/25	30		0.84	3.45	9.04	17.7	29.9	41.5	47.4	59.2			
1/31	40		0.84	2.90	6.34	15.0	24.1	37.9	47.4	65.3	78.4	91.4	104
2/12	40			2.80	8.31	16.7	27.7	45.7	58.2	81.9	98.3	122	140
2/15	40			2.08	6.11	10.8	15.5	21.0	30.1	48.0	59.8	69.8	79.8

Table 10. Soil moisture tension gradients at several tensions by dates in cylinder B

Date	Temp. °C	Soil moisture tension (cm H2O)											
		30	50	75	100	125	150	175	200	250	300	350	400
		Soil moisture tension gradient (cm H2O/cm)											
3/23/62	40	0.462	2.69	5.55	7.97								
3/24	40	0.402	2.78	7.27	11.02								
3/29	30	0.462	3.32	7.58									
4/2	30	0.402	2.98	7.91									
4/6	20	0.587	3.98	8.26									
4/11	20	0.402	3.98	7.91									
4/20	12	0.619	3.69	8.64									
5/22	30						4.32	5.14	5.98	7.77	13.8	19.9	25.4
5/25	30							4.65	5.43	7.77	12.4	20.3	25.4
7/1	20						5.40	6.53	7.73	12.35	17.1	23.0	27.3
7/28	12						5.20	6.99	8.29	10.74	15.3	23.0	31.9
11/15	12	0.766	1.74	6.23	10.34	13.90	21.3	28.1	32.1	41.5	49.8	60.2	68.8
11/20	12	0.966	1.80	3.77	9.44	14.25	21.3	24.8	28.4	36.5	45.2	52.7	60.3
11/22	12	1.12	2.07	3.97	10.34	15.00	19.0	22.2	25.3	35.4	42.5	51.1	60.3
11/29	12		1.61	4.42	7.67	15.82	22.6	28.1	32.1	40.2	53.2	62.0	70.9
12/11	20		1.28	3.97	7.67	15.00	24.9	30.1	34.4	43.0	51.6	60.2	68.8
12/14	20		1.93	4.12	8.31	16.26	25.8	31.2	35.6	44.5	53.4	62.3	71.2
12/27	20			2.70	4.94	9.58	16.3	23.4	32.1	40.2	48.2	56.2	64.2
12/29	20			2.16	5.21	9.21	16.3	24.1	30.1	40.2	51.6	62.3	73.9
1/3/63	20		1.33	4.12	5.90	10.83	18.0	23.4	32.1	48.0	57.6	67.2	76.7
1/18	30			3.58	5.90	11.30	18.0	25.6	32.1	43.0	53.4	64.7	79.8
1/22	30		1.50	3.84	6.58	12.63	18.0	24.8	34.4	46.2	57.6	67.2	76.7
1/25	30			3.70	6.34	10.83	20.1	30.1	43.3	59.2	74.6	91.4	104.5
1/31	40		1.12	3.34	8.66	15.82	24.1	34.9	41.6	54.2	65.0	75.8	86.7
2/15	40		1.07	3.70	7.98	12.93	16.3	20.0	24.0	37.7	48.2	56.2	64.2

Table 11. Soil moisture tension gradients at several tensions by dates in cylinder C

| Date | Temp. °C | Soil moisture tension (cm H_2O) | | | | | | | | | | | |
		50	75	100	125	150	175	200	250	300	350	400	500
		Soil moisture tension gradient (cm H_2O/cm)											
3/23/62	40	3.20	7.91	12.1	17.5								
3/24	40	3.20	7.91	12.1	17.5								
3/29	30	3.70	9.98	14.0	18.5								
4/2	30	4.47	10.50	41.8									
4/6	20	6.00	12.46	17.2									
4/20	12	4.94	12.05	16.6									
5/3	40			3.23	4.18	5.40	9.61	14.2	24.7	34.2	42.0	48.8	63.3
5/22	30					2.38	3.93	6.21	14.7	21.3	25.8	29.5	36.8
5/25	30						3.76	4.90	11.1	21.3	25.8	29.5	26.8
11/15	12	1.50	4.42	7.67	12.9	17.1	21.0	24.0	30.0	36.0	42.0	48.0	60.0
11/20	12	1.33	2.90	6.11	8.87	14.8	21.0	25.3	31.6	38.0	44.3	50.6	63.3
11/22	12	2.38	3.70	5.30	9.58	17.1	20.5	24.0	30.0	36.0	42.0	48.0	60.0
11/29	12	2.15	3.34	6.58	11.8	18.5	22.2	25.3	31.6	38.0	44.3	50.6	63.3
12/11	20	1.61	4.12	6.58	11.8	19.0	23.4	27.5	35.4	42.5	49.6	56.7	70.9
12/14	20	1.80	3.11	7.37	12.4	17.1	21.0	25.3	33.4	40.1	46.8	53.5	66.9
12/27	20		1.40	3.73	5.96	12.5	19.0	24.0	31.6	39.0	45.5	52.0	65.0
12/29	20		1.61	4.15	7.37	10.6	18.1	21.7	28.5	36.0	44.2	52.0	66.9
1/3/63	20		3.70	5.30	7.37	13.6	20.0	24.0	31.6	40.1	46.8	53.5	66.9
1/18	30		2.08	4.94	8.22	14.2	20.0	24.0	30.8	39.0	46.8	53.5	66.9
1/22	30		2.80	5.49	7.37	11.5	19.0	25.3	32.5	40.1	46.8	55.1	70.9
1/25	30		2.42	5.09	10.4	14.8	19.0	24.0	33.4	42.5	52.7	60.3	77.8
1/31	40		2.42	5.69	8.54	15.5	21.0	25.3	31.6	38.0	44.3	50.6	63.3
2/15	40		2.80	5.49	9.58	17.1	21.0	28.4	40.2	55.4	64.7	73.9	92.4

Table 12. Soil moisture tension gradients at several tensions by dates in cylinder D

Date	Temp. °C	Soil moisture tension (cm H₂O)											
		100	125	150	175	200	225	250	275	300	325	350	400
		Soil moisture tension gradient (cm H₂O/cm)											
3/23/62	40	2.99	5.96	9.17	15.5	21.2	27.0	33.4	37.9	42.5	47.5	52.7	60.3
3/24	40	2.99	5.96	9.17	15.5	21.2	27.0	33.4	37.9	42.5	47.5	52.7	60.3
3/29	30	3.11	6.39	8.84	14.5	23.4	30.1	37.7	44.2	49.8	55.9	62.3	71.2
4/2	30	3.11	6.39	8.84	14.5	23.4	30.1	37.7	44.2	49.8	55.9	62.3	71.2
4/6	20	2.50	5.09	10.64	16.2	22.8	28.5	34.4	39.0	42.5	46.1	51.1	58.4
4/11	20	2.50	2.09	10.64	16.2	22.8	28.5	34.4	39.0	42.5	46.1	51.1	58.4
4/20	12	2.55	5.37	8.53	13.7	18.9	24.4	30.8	35.8	40.1	44.7	49.6	71.2
5/3	40				4.47	8.29	10.4	12.8	17.4	23.0	27.6	34.6	48.0
5/22	30					5.11	7.81	11.5	14.6	18.3	21.4	24.4	30.7
5/25	30					5.21	8.39	12.4	13.8	16.5	19.2	23.9	29.5
7/1	20			3.52	4.29	5.98	9.01	12.4	15.6	19.7	23.0	26.8	33.2
7/8	20					4.30	5.28	7.48	10.6	14.3	16.6	18.6	21.2
7/13	12			3.37	4.29	6.45	8.10	11.4	13.1	15.1	18.5	23.9	39.5
7/28	12			2.51	3.93	6.94	9.33	12.4	15.6	19.0	22.2	25.8	33.2
11/15	12	2.55	4.83	8.84	12.0	14.7	17.2	12.2	26.0	29.0	32.1	34.6	39.5
11/20	12	1.96	4.02	7.64	11.1	14.2	16.3	18.4	21.9	25.4	29.4	33.0	43.4
11/22	12	2.35	4.02	8.23	12.0	14.2	16.3	18.4	21.1	26.0	29.4	30.0	39.5
11/29	12	2.88	5.18	9.17	12.4	14.7	18.0	20.8	22.8	24.9			
12/11	20	2.77	5.76	9.87	13.4	16.0	19.5	23.6	27.2	32.6	36.1	39.9	45.6
12/14	20	2.77	7.11	11.06	13.4	15.6	18.0	20.4	23.8	29.6	35.3	39.9	49.3
12/29	20	2.66	3.60	5.59	8.64	10.6	12.8	17.1	21.9	26.0	30.7	36.2	45.6
1/3/63	20	2.99	4.18	6.44	8.95	11.4	15.4	19.6	24.3	29.0	32.1	38.0	45.6
1/18	30	2.35	4.18	7.41	9.61	11.4	14.8	19.2	23.8	29.6	33.6	38.9	45.6
1/22	30	2.77	4.18	7.15	10.7	12.7	14.3	20.0	24.9	29.6	33.6	38.9	45.6
1/25	30	1.96	4.02	6.91	10.3	12.7	14.3	17.7	21.9	28.3	35.3	44.3	56.7
2/12	40	1.68	3.46	6.91	9.61	11.4	13.0	15.8	20.3	27.1	35.3	42.0	56.7
2/13	40		2.93	6.01	8.64	10.4	12.6	15.3	18.8	23.0	30.7	38.0	56.7
2/15	40	2.05	3.32	6.67	8.95	11.0	12.8	15.8	18.8	23.9	29.4	36.2	53.5

73

Table 13. Soil moisture conductivity coefficients at several tensions and temperatures by dates in cylinder A

Date	Temp. °C	Soil moisture tension (cm H₂O)											
		30	50	75	100	125	150	175	200	250	300	350	400
		Soil moisture conductivity (microns per day)											
3/23/62	40	10690	1340										
3/24	40	14050	1400										
3/29	30	6500	1050										
4/2	30	10550	1350										
4/6	20	3890	871										
4/11	20	5980	954										
4/20	12	4380	761										
5/3	40				205	155	62.4	32.6	20.3	11.4	1.10	6.55	5.39
5/22	30						69.9	31.3	18.0	7.85	5.38	4.33	3.71
5/25	30						77.7	37.5	20.6	9.72	6.56	5.08	4.21
7/1	20					54.4	43.3	29.0	19.6	9.55	6.35	4.61	3.86
7/28	12					69.8	55.9	46.1	34.7	19.5	12.6	10.1	8.18
11/15	12		231	62.3	26.3	15.5	12.0	9.54	8.34	6.15			
11/20	12		370	88.8	34.9	20.1	13.7	10.9	9.50				
11/22	12		379	92.1	33.5	22.6	15.6	8.88	7.23				
11/29	12			113	36.7	19.3	12.7	9.43	7.64	6.11			
12/11	20		146	47.0	18.2	9.9	7.48	6.41	5.03				
12/14	20		311	81.5	33.7	21.7	15.2	13.0	10.9				
12/27	20			91.8	30.2	15.2	9.12	6.37	5.16	3.80			
12/29	20			99.7	29.0	13.4	8.98	6.79	5.55	4.14			
1/3/63	20		505	240	102	47.2	27.9	20.8	14.2	10.3			
1/18	30		824	319	152	68.3	41.0	26.5	21.4	14.2			
1/22	30		701	281	153.	71.5	37.6	23.4	16.7	10.3			
1/25	30		1003	243	93.0	47.5	28.1	20.3	17.7	14.2			
1/31	40		1325	383	175	74.0	46.1	29.3	23.4	17.0	14.2	12.1	10.6
2/12	40			276	92.9	46.2	27.8	16.9	13.3	9.42	7.85	6.30	5.51
2/15	20			386	131	74.0	51.6	38.1	26.6	16.7	13.4	11.5	10.1

Table 14. Soil moisture conductivity coefficients at several tensions and temperatures by dates in cylinder B

Date	Temp. °C	Soil moisture tension (cm H_2O)											
		30	50	75	100	125	150	175	200	250	300	350	400
		Soil moisture conductivity (microns per day)											
3/23/62	40	10600	1820	883	615								
3/24	40	11540	1670	638	421								
3/29	30	7700	1070	470									
4/2	30	9150	1230	465									
4/6	20	4580	675	326									
4/11	20	7060	713	359									
4/20	12	3300	552	236									
5/22	30						33.8	28.4	24.4	18.8	10.6	7.34	5.75
5/25	30							22.6	19.4	13.5	8.43	5.17	4.13
7/1	20						26.3	21.8	18.4	11.5	8.32	6.17	5.20
7/28	12						21.3	15.3	12.9	10.0	6.97	4.65	3.35
11/15	12	355	157	43.6	26.3	19.6	12.8	9.68	8.46	6.55	5.46	4.52	3.95
11/20	12	231	124	59.2	23.6	15.6	10.5	8.99	7.86	6.11	4.93	4.23	3.70
11/22	12	245	132	68.9	26.5	18.3	14.4	12.4	10.8	7.73	6.44	5.36	4.54
11/29	12		202	73.7	42.5	20.6	14.4	11.6	10.1	8.12	6.13	6.42	4.60
12/11	20		349	112	58.2	29.8	18.0	14.8	13.0	10.4	8.66	7.42	6.50
12/14	20		199	93.5	46.3	23.7	14.9	12.4	10.8	8.64	7.20	6.18	5.40
12/27	20			93.0	50.8	26.2	15.4	10.3	7.81	6.25	5.21	4.47	3.91
12/29	20			121	50.3	28.4	16.1	10.9	8.70	6.52	5.08	4.20	3.54
1/3/63	20		365	118	82.4	44.9	27.0	20.8	15.1	10.1	8.44	7.23	6.33
1/18	30			223	135	70.6	44.3	31.2	24.8	18.6	14.9	12.3	10.0
1/22	30		628	245	144	74.7	52.4	38.0	27.4	20.4	16.4	14.0	12.3
1/25	30			216	126	73.8	39.9	26.6	18.4	13.5	10.7	8.75	7.66
1/31	40		895	301	116	63.5	41.7	28.8	24.2	18.6	15.4	13.2	11.6
2/15	40		667	193	89.7	55.4	44.0	35.9	29.8	19.0	14.9	12.7	11.2

Table 15. Soil moisture conductivity coefficients at several tensions and temperatures by dates in cylinder C

Date	Temp. °C	Soil moisture tension (cm H_2O)											
		50	75	100	125	150	175	200	250	200	350	400	500
		Soil moisture conductivity (microns per day)											
3/23/62	40	1670	678	444	306								
3/24	40	1620	657	430	297								
3/29	30	1040	384	274	207								
4/2	30	852	363	258									
4/6	20	488	235	170									
4/20	12	466	191	138									
5/3	40			387	299	232	130	88.1	50.6	36.5	29.8	25.6	19.8
5/22	30					127	77.1	48.8	20.6	14.2	11.7	10.3	8.22
5/25	30						63.8	49.0	21.6	11.3	9.30	8.14	6.51
11/15	12	211	71.5	41.2	24.4	18.5	15.0	13.2	10.5	8.78	7.52	6.58	5.27
11/20	12	231	106	50.2	34.6	20.7	14.6	12.1	9.70	8.09	6.93	6.06	4.85
11/22	12	151	96.9	67.7	37.5	21.0	17.5	15.0	12.0	9.97	8.55	7.48	5.98
11/29	12	185	119	60.5	33.7	21.5	18.0	15.7	12.6	10.5	8.98	7.86	6.29
12/11	20		105	65.5	36.5	22.7	18.4	15.7	12.2	10.1	8.69	7.60	6.08
12/14	20		160	67.6	40.4	29.2	23.8	19.7	14.9	12.4	10.7	9.32	7.46
12/27	20		249	93.2	58.3	27.9	18.3	14.5	11.0	8.91	7.65	6.68	5.35
12/29	20		256	99.3	55.9	38.7	22.8	19.0	14.4	11.4	9.32	7.91	6.16
1/3/63	20		169	118	85.0	46.2	31.4	26.1	19.8	15.6	13.4	11.7	9.36
1/18	30		395	166	99.7	57.9	41.1	34.2	26.6	21.0	17.5	15.3	12.3
1/22	30		315	161	120	76.7	46.4	34.8	27.1	22.0	18.8	16.0	12.4
1/25	30		317	151	73.9	51.8	40.4	32.0	23.0	18.1	14.6	12.7	9.87
1/31	40		368	157	104	57.4	42.4	35.0	28.2	23.5	20.1	17.6	14.1
2/15	40		472	240	138	77.2	62.8	46.6	32.9	23.8	20.4	17.9	14.3

Table 16. Soil moisture conductivity coefficients at several tensions and temperatures in cylinder D

Date	Temp. °C	Soil moisture tension (cm H$_2$O)											
		100	125	150	175	200	225	250	275	300	325	350	400
		Soil moisture conductivity (microns per day)											
3/23/62	40	4700	2360	1530	906	662	520	420	370	330	296	266	233
3/24	40	4810	2410	1568	928	678	533	431	379	338	303	273	238
3/29	30	3570	1740	1260	764	475	369	295	252	223	199	178	156
4/2	30	3620	1760	1270	777	482	374	299	255	226	202	181	158
4/6	20	3650	1790	857	563	400	320	265	234	215	198	178	156
4/11	20	3480	1710	819	538	382	306	253	223	205	189	170	149
4/20	12	3010	1430	899	561	406	314	249	214	191	172	154	108
5/3	40				1190	640	512	415	305	231	192	154	111
5/22	30					628	411	279	220	175	150	132	105
5/25	30					626	382	264	236	198	170	136	110
7/1	20				515	370	245	179	141	112	96	82	66
7/8	20					360	294	207	146	108	93	84	73
7/13	12			706	542	369	294	209	181	158	129	100	60
7/28	12			860	550	311	232	175	138	114	97	84	65
11/15	12	1540	816	446	330	267	228	186	152	136	123	114	100
11/20	12	1780	866	455	314	245	214	189	159	137	118	105	80
11/22	12	1610	940	459	316	266	232	205	179	145	129	114	96
11/29	12	1320	736	415	307	258	212	183	167	153			
12/11	20	1690	811	473	348	293	240	198	172	143	129	117	102
12/14	20	1730	672	432	356	306	266	235	201	161	135	120	97
12/29	20	1800	1330	859	556	453	375	281	219	185	156	133	105
1/3/63	20	1860	1330	865	622	489	363	285	229	192	173	147	122
1/18	30	2910	1640	923	712	601	462	357	287	231	204	176	150
1/22	30	2530	1680	982	656	554	492	352	282	237	209	180	154
1/25	30	3360	1640	952	638	519	461	371	300	232	186	149	116
2/12	40	4060	1970	987	710	599	523	430	336	252	193	162	120
2/13	40		2280	1110	774	643	532	438	356	291	218	176	118
2/15	40	3360	2080	1030	770	628	538	435	367	288	234	190	129

Appendix III.   Tension as a function of temperature
and moisture content

Moisture content of the three soils at different moisture tensions
and temperatures are given in Tables 6, 7, and 8. The Utah State Univer-
sity IBM 1620 was utilized to make separate multiple regression analyses
for each soil using the data in these tables. Several different combina-
tions and transformations were tried in an equation of the type:

$$y = \beta_o + \sum_1^h \beta_m x_m \qquad (37)$$

The following equations were accepted because they fit the data well:

1) Subalpine clay loam:

$$\log\tau = 5.45274 - 0.081713x_1 - 0.0052801x_2 - 0.00011101x_1x_2$$
$$- 0.0000031720x_1^2 + 0.000097057x_2^2 \qquad (38)$$

in which τ is soil moisture tension in centimeters of water, x_1 is mois-
ture content percentage by weight, and x_2 is temperature (degrees
Celsius). This equation accounts for 97.4 percent of the variation in
$\log\tau$ in the subalpine soil.

2) Mountain brush zone clay loam:

$$\log\tau = 10.61737 - 0.37032x_1 - 0.0062885x_2 - 0.00014856x_1x_2$$
$$+ 0.000095374x_1^3 + 0.15423 \log x_2 \qquad (39)$$

The variables in this equation are the same as those in equation
(38). This equation accounts for 98.0 percent of the variation in $\log\tau$
in the mountain brush soil.

3) Millville silt loam:

$$\tau = 6030 + 382x_1 - 7.02x_1^2 + 1.575T +$$
$$(18697 - 67.78T + 0.40805T^2)(x - 7.663)^{-1} \qquad (40)$$

The variables x_1 and x_2 in this equation are also P_w and Celsius temperature, respectively. This equation accounts for 98.5 percent of the variation in τ.

These three equations were evaluated at 12°, 20°, 30°, and $40^\circ C$ over the range of moisture contents involved in this study. The estimated tensions so obtained for these temperatures and moisture contents in the three soils are listed in Table 17.

Table 17. Soil moisture tension at four temperatures
at several moisture contents in the three
soils

Moisture content	Soil moisture tension			
	12°C	20°C	30°C	40°C
% by wt.	centimeters of water equivalent suction			

Subalpine clay loam

33	354	318	289	275
34	285	256	232	220
35	230	205	186	176
36	184	164	149	140
37	148	132	119	112
38	118	105	95	89
39	95	84	75	71
40	76	67	60	56

Brush zone clay loam

26	509	460	388	321
27	346	309	260	214
28	242	216	180	148
29	175	156	130	107
30	132	117	97	79
31	103	92	76	62
32	84	74	62	50
33	72	63	52	41
34	64	56	46	37

Millville silt loam

17	376	345	310	283
18	326	299	269	247
19	294	272	246	227
20	274	254	232	216
21	259	242	222	208
22	245	230	213	201
23	229	216	201	191
24	209	198	185	176
25	184	174	162	156
26	151	143	133	127

Appendix IV. Conductivity as a function of temperature and moisture content

Soil moisture conductivity coefficients were determined at various soil moisture tensions and temperatures and presented in Appendix II. These coefficients can also be expressed in terms of moisture content instead of tension by using the moisture tension-moisture content relations in Appendix III. The procedure consists of the following two steps:

Step 1. All of the conductivity coefficients for a particular temperature, cylinder and period, are plotted on log-log graph paper with tension as the independent variable. Separate curves for cylinders A, B, and C during periods I and III and for cylinder D during all three periods were fitted to these data. Some of these curves are shown in Figures 6 through 10.

Step 2. Table 17 lists the soil moisture tensions at each of the four temperatures at several moisture contents. For any particular moisture content, the conductivity coefficients at each of the four temperatures can be obtained from the curves obtained in Step 1 by reading the conductivity coefficient for the temperature of interest at the tension given in Table 17 for that temperature and moisture content. For example, according to Table 17 the subalpine soil at a moisture content of 37 percent has a tension of 148 cm water at $12^{\circ}C$. The $12^{\circ}C$ curve for cylinder A shown in Figure 6 indicates a conductivity of $13.8\mu/day$ at this tension. At $40^{\circ}C$ the moisture tension in the same soil at 37 percent P_w is only 112 cm water; the $40^{\circ}C$ curve in Figure 6 indicates a conductivity of $90\mu/day$ at this tension. All of the conductivity coefficients in Tables 18, 19, and 20 were calculated in a similar fashion.

Table 18. Soil moisture conductivity coefficients of the subalpine clay loam at four temperatures at several moisture contents

P_w	Soil moisture conductivity			
	12°C	20°C	30°C	40°C
%	- - - - - microns per day - - - - -			

Cylinder A - Period I

P_w	12°C	20°C	30°C	40°C
41	600	834	1305	1735
42	781	1275	2310	3790

Cylinder A - Period III

P_w	12°C	20°C	30°C	40°C
34	3.9	5.8	14	17
35	6.0	7.6	21	27
36	9.2	11.2	36	46
37	13.8	18.2	74	90
38	21.6	33.1	150	185
39	38.5	76.0	280	440
40	89.0	140	540	950

Cylinder B - Period I

P_w	12°C	20°C	30°C	40°C
40	245	405	710	1306
41	349	603	1370	2520
42	620	1200	3250	6620

Cylinder B - Period III

P_w	12°C	20°C	30°C	40°C
33	4.9	6.7	15	17
34	6.2	8.2	19	23
35	7.8	10.6	28	32
36	10.2	15.1	43	47
37	13.5	24.0	83	76
38	19.4	47.5	143	153
39	31.2	87	230	310
40	61.0	154	380	610

Table 19. Soil moisture conductivity coeffi-
cients of the mountain brush zone
clay loam at four temperatures at
several moisture contents

P_W	Soil moisture conductivity			
	12°C	20°C	30°C	40°C
%	- - - - -	microns per day	- - - - -	

Period I

31	318	186	370	938
32	170	229	577	1620
33	206	279	839	3550
34	269	358	1220	4510

Period III

26	5.6	6.8	15	21
27	8.0	10.8	25	36
28	11.5	17	40	73
29	16.5	29	91	191
30	25.5	66	170	305
31	50.5	112	305	700

Table 20. Soil moisture conductivity coeffi-
cients of Millville silt loam at
four temperatures several moisture
contents

P_w	Soil moisture conductivity			
	12°C	20°C	30°C	40°C
%	- - - - - microns per day - - - - - -			

Period I

17	139	177	212	363
18	169	208	281	440
19	195	232	309	516
20	216	253	343	570
21	239	271	380	615
22	264	293	418	660
23	302	331	481	740
24	368	296	600	910
25	488	565	890	1240
26	810	1020	1550	2300

Period II

17	75	85	171	275
18	110	112	234	403
19	140	148	283	497
20	164	181	346	565
21	183	211	410	620
22	207	246	485	680
23	239	296	620	780
24	296	370	890	1020

Period III

17	95	133	217	330
18	114	172	302	445
19	146	210	370	515
20	164	243	416	560
21	179	270	455	595
22	194	300	490	625
23	212	339	548	680
24	242	390	625	765
25	292	482	810	950
26	440	735	1350	1950

Appendix V. Regression methods used to
calculate activation energy coefficients

The coefficient b defined by equation (30):

$$b = - \frac{d \ln \lambda}{d(T^{-3})} \tag{30}$$

was calculated for each moisture content in each cylinder using all of
the conductivity coefficients tabulated in Appendix IV. The simple
linear regression equation was used:

$$\ln \lambda = \beta_o + \beta_1 T^{-3} \tag{41}$$

The regression coefficient β_1 is equivalent to -b because the
differential of equation (41) is:

$$d \ln \lambda = \beta_1 d(T^{-3}) \tag{42}$$

There was no significant covariance of the regression coefficients
with moisture content or period of measurement in any one cylinder, nor
were there any significant differences between cylinders A and B which
both contained the same subalpine soil. Accordingly, the data were
pooled and an average regression coefficient calculated for each soil,
and 95 percent confidence limits were calculated from the pooled variance
of individual observations from regression equations containing the
average regression coefficient in common.

The b coefficient is related to activation energy in the following
way. Activation energy of liquid flow is defined by the equation:

$$E_a = RT^2 \frac{d \ln \lambda}{dT} \tag{12a}$$

Since $d(T^{-3}) = -3T^{-4}dT$, equation (30) may be written:

$$b = - \frac{d \ln \lambda}{d(T^{-3})} = \frac{T^4}{3} \frac{d \ln \lambda}{dT} \qquad (30a)$$

Therefore

$$E_a = 3RbT^{-2} \qquad (43)$$

Appendix VI. Propositions

As a part of his final examination, each Ph.D. candidate in the Agronomy Department of Utah State University must devise at least eight propositions and be prepared to defend those elected by his committee and the Agronomy Department staff. This appendix contains the descriptions and arguments of the three propositions presented on April 15, 1964.

Proposition 1. The disparity between total potential and zeta potential, which is ordinarily explained by the slippage plane concept, can be ascribed to viscosity variations of the liquid in the colloid's electrostatic field.

The distribution of electrical potential adjacent to the surface of a charged colloid can be described by a curve similar to:
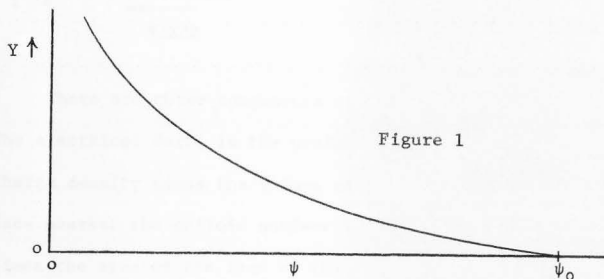
Figure 1

The magnitude of the potential is ψ_o (total potential) at the colloid surface and decreases with distance (Y) from the surface, usually approaching zero exponentially. The exact shape of this curve is not important for present purposes. The only assumption made in this regard is that it satisfies Poisson's equation

$$\nabla^2 \psi = - \frac{4\pi\rho}{\epsilon} \qquad (A-1)$$

which is a general equation relating the change in potential gradient to space charge density ρ (the sum of ionic charges per unit volume) and dielectric constant, ϵ, of the fluid (Harnwell, 1938).

If an electric field, E, is applied to the fluid while the colloid is held stationary, the forces on any element of fluid at distance Y from the surface will consist of electric and viscous forces whose resultant is zero at steady state which will be attained in a relatively short period of time.
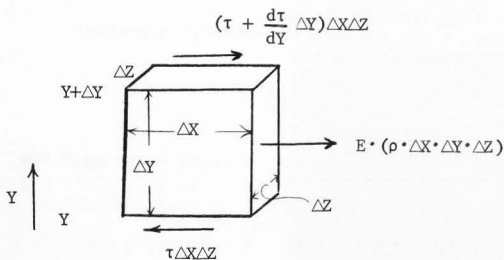
There are three components of force on this fluid element (Figure 1). The electrical force is the product of the electric field times the space charge density times the volume of the element. $E \cdot \rho \cdot \triangle X \cdot \triangle Y \cdot \triangle Z$. On the face nearest the colloid surface Y, the force is the shear stress (τ) times the area of the face of the element and retards movement of the element: $- \tau \triangle X \triangle Z$. At the other side of the element, $Y + \triangle Y$, the force is positive with respect to E and is the product of the area of the face of the element and the shear stress at $Y + \triangle Y$ which is τ at Y plus $\frac{d\tau}{dY} \triangle Y$: $(\tau + \frac{d\tau}{dY} \triangle Y) \triangle X \triangle Z$.

At steady state the sum of these forces are zero and therefore:

$$\tau \triangle X \triangle Z = (\tau + \frac{d\tau}{dY} \triangle Y) \triangle X \triangle Z + E \rho \triangle X \triangle Y \triangle Z \qquad (A-2)$$

If we divide both sides by $\triangle X \triangle Y \triangle Z$ we obtain

$$\frac{\tau}{\triangle Y} = \frac{\tau}{\triangle Y} + \frac{d\tau}{dY} + E\rho \tag{A-3}$$

Subtracting $\frac{\tau}{\triangle Y}$ from both sides and rearrange (A-3) we get

$$\rho\,dY = - E d\tau \tag{A-4}$$

Poisson's equation in one dimension may be written:

$$\frac{d}{dY} \left(\frac{d\psi}{dY}\right) = - \frac{4\pi}{\varepsilon} \rho \tag{A-5}$$

and rearranged to:

$$\rho\,dY = - \frac{\varepsilon}{4\pi} d \left(\frac{d\psi}{dY}\right) \tag{A-6}$$

Equating (A-4) to (A-6) yields

$$E d\tau = \frac{\varepsilon}{4\pi} d \left(\frac{d\psi}{dY}\right) \tag{A-7}$$

The indefinite integral of which is

$$\tau = \frac{E\varepsilon}{4\pi} \frac{d\psi}{dY} + c \tag{A-8}$$

According to Newton's definition of viscosity (Albertson, Barton, and Simons, 1960), shear stress is proportional to the velocity gradient, the proportionality constant (η) being viscosity:

$$\tau = \eta \frac{dv}{dY} \tag{A-9}$$

Equating (A-8) and (A-9) yields

$$\eta \frac{dv}{dY} = \frac{E\varepsilon}{4\pi} \frac{d\psi}{dY} + c \tag{A-10}$$

For this equation we have the following boundary conditions: when Y is large both the potential gradient and the velocity gradient are negligible:

$$\text{at } Y \to \infty \quad \frac{d\psi}{dY} \to Q, \quad \frac{dv}{dY} \to 0$$

therefore c of equation (A-10) is negligibly small and can be ignored.

If we multiply both sides by $\frac{\eta}{dY}$ we obtain:

$$dv = \frac{E\varepsilon}{4\pi\eta} \, d\psi \tag{A-11}$$

The integral of this from Y = 0 to Y $\to$ ∞ is

$$\int_0^{v_E} dv = \frac{E}{4\pi} \int_{\psi_0}^{0} \frac{\varepsilon}{\eta} \, d\psi \tag{A-12}$$

v_E is velocity a large distance from the colloid surface. Both ε and η must be placed inside the integral sign because we have no assurance that they are independent of ψ. Equation (A-12) integrates to:

$$v_E = \frac{E}{4\pi} \int_{\psi_0}^{0} \frac{\varepsilon}{\eta} \, d\psi \tag{A-13}$$

We cannot integrate the right hand side of equation (A-13) without making some assumptions about η and ε. The assumption usually made is based on the slippage plane concept, which in effect, states that the viscosity of the fluid is infinite out to a slippage plane where the potential is ζ (of lesser magnitude than ψ_0) but that beyond this plane the viscosity is the same as that of free water. It is also assumed that ε beyond the slippage plane is the same as that of free water. When these assumptions are incorporated equation (A-13) may be written:

$$\frac{4\pi v_E}{E} = \int_{\psi_0}^{\zeta} \frac{\varepsilon}{\infty} \, d\psi + \frac{\varepsilon_0}{\eta_0} \int_{\zeta}^{0} d\psi \tag{A-14}$$

which integrates to:

$$\frac{4\pi v_E}{E} = - \frac{\epsilon_o}{\eta_o} \zeta \qquad (A-15)$$

This is the classical equation for electro-osmotic velocity (Overbeek, 1952). The subscript o indicates free-water values.

However, there is a growing body of evidence that viscosity increases as charged colloid surfaces are approached (Rosenqvist, 1959; Kunze and Kirkham, 1961; Wu, 1964), but this is a gradual change and not an abrupt change from normal free-water viscosity to infinite viscosity as assumed in the slippage plane concept.

If we assume for the present that ϵ is independent of ψ but that η is a function of ψ, we can rewrite equation (A-13) as follows:

$$v_E = \frac{E \epsilon_o}{4\pi \eta_o} \int_{\psi_o}^{o} \frac{\eta_o}{\eta} \, d\psi \qquad (A-16)$$

Comparing this with equation (A-15) we see that:

$$\zeta = - \int_{\psi_o}^{o} \frac{\eta_o}{\eta} \, d\psi \qquad (A-17)$$

This equation shows that an observed value of ζ less than ψ_o is the consequence of values of η being greater than η_o close to colloid surfaces.

Literature Cited

Albertson, M. L., J. R. Barton, and D. B. Simons. 1960. Fluid mechanics for engineers. Prentice-Hall, Inc., Englewood Cliffs, N.J. p. 202-203.

Harnwell, G. P. 1938. Principles of electricity and electromagnetism. McGraw-Hill Book Co., Inc. N.Y. p. 30.

Kunze, R. J. and D. Kirkham. 1961. Deuterium and the self-diffusion coefficient of soil water. Soil Sci. Soc. Am. Proc. 25: 9-12.

Overbeek, J. Th. G. 1952. Electrokinetic phenomena, p. 194-244. In Colloid Science Vol. I, H. R. Kruyt, ed. Elsevier Publishing Co. Amsterdam.

Rosenqvist, I. Th. 1959. Physico-chemical properties of soils: soil water systems. J. Soil Mechanics and Foundations Div. Amer. Soc. Civil Eng. 85(SM2): 31-53.

Wu, T. H. 1964. A nuclear magnetic resonance study of water in clay. J. Geophys. Research 69: 1083-1091.

Proposition 2. The effects of subalpine range reseeding on watershed condition can be predicted on the basis of pretreatment measurements of soil and vegetation conditions.

The severe climate of the subalpine range causes a delicate balance in soil-plant relations. The growing season is short and even under optimum conditions plant development is scarcely greater than is necessary to hold the soil in place and prevent flash floods.

When some harsh treatment such as heavy grazing, fire, or cultivation is imposed on these lands the delicate balance is disturbed and watershed condition may be damaged. Watershed condition is defined here as an integration of soil stability, flood potential and all the related environmental factors. A watershed in good condition has porous soil so that infiltration capacity is great enough to absorb high-intensity rainfall just about as fast as it falls to prevent excessive overland flow. It must also have a well-distributed vegetation cover to protect and maintain good soil conditions.

When subalpine range is subjected to grazing impact, or some other disruptive influence, soil porosity and vegetation are usually reduced to some extent. If the impact is severe enough, soil erosion becomes excessive and watershed condition declines. Unless corrective action is taken the damaged area eventually becomes badly eroded and a potential flood source.

Reseeding serves a dual purpose. It is employed to increase vegetation on damaged sites and to improve species composition. Occasionally some subalpine range in satisfactory watershed condition is reseeded to produce more palatable forage for livestock. In either case, the treatment affects watershed condition to some extent.

It is proposed here that these effects of seeding on watershed condition can be predicted on the basis of pretreatment site conditions. Two steps are involved in the discussion in favor of this proposition. First, it is proposed that watershed condition can be estimated on the basis of soil and vegetation conditions alone; that is, flood potential and soil stability depend on soil and vegetation and can be predicted if the characteristics of these site factors are known. Second, if enough is known about a site, the response of its soil and vegetation to seeding treatment can be predicted.

We have little information available on either point that applies to subalpine conditions. A rigorous proof cannot be given at present but the results of studies in central Utah are given for illustrative purposes.
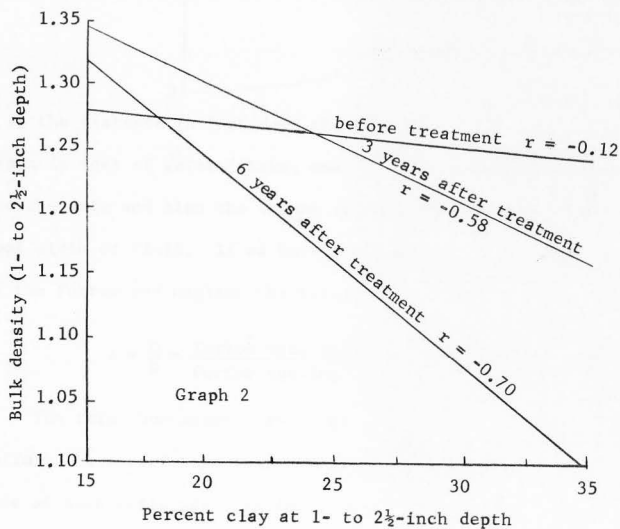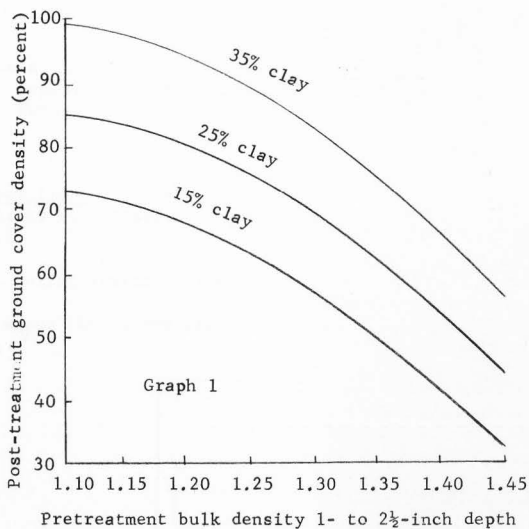
An infiltrometer study on subalpine cattle range in central Utah (Meeuwig, 1960) serves to illustrate the first point. Multiple regression analyses showed that the amount of water retained on plots and the amount of soil eroded from these plots during a simulated high-intensity rainstorm could be predicted from the density of plant and litter cover on the plot and the bulk density of the surface 4 inches. Water retained and soil eroded are good indices of flood potential and soil stability, respectively. The indicated cover and soil properties accounted for 75 percent of the variance of each of these two variables. By means of graphs these two variables can be predicted with reasonable accuracy from

the cover and soil properties.

In regard to the second point, it seems reasonable to expect that cultivation under a given set of conditions of a soil with a given set of properties will have a predictable effect on soil bulk density. And, if nothing unusual happens, a certain amount of vegetative cover will eventually become associated with this given set of soil and climatic conditions. We have even less information available on this point. However, another study in the subalpine zone of central Utah, the results of which are as yet unpublished, serves to illustrate this second point. It was found here that plant and litter cover six years after reseeding was closely related to soil texture and pretreatment bulk density. This relation is shown in Graph 1. While the correlation is not exceptionally high ($r = 0.68$), it is significant at the 1-percent level and supports the hypothesis advanced here.

The effects of seeding on bulk density are also influenced by day content. More precisely, the cultivation tends to erase the impact of past use on bulk density so that a definite relation between clay content and bulk density emerge. Graph 2 illustrates this. Before treatment there was no significant relation between clay content and bulk density because variable past grazing history obscured any natural relations. Three years after seeding a significant correlation was apparent, and six years after seeding this correlation was highly significant.

These two examples support the hypothesis that post-treatment cover and soil conditions can be predicted from pretreatment soil conditions and, therefore, any changes in these conditions due to treatment can be predicted; and these predicted changes can be used in turn to predict treatment effects on flood potential and soil stability.

Graph 1

Post-treatment ground cover density (percent)

35% clay

25% clay

15% clay

Pretreatment bulk density 1- to 2½-inch depth

Graph 2

Bulk density (1- to 2½-inch depth)

before treatment   r = -0.12

3 years after treatment
r = -0.58

6 years after treatment   r = -0.70

Percent clay at 1- to 2½-inch depth

Literature Cited

Meeuwig, R. O. 1960. Effects of seeding and grazing on infiltration capacity and soil stability on a subalpine range in central Utah. Unpublished MS thesis. University of California Library, Berkeley.

Proposition 3. Water intake during furrow irrigation on homogeneous soils is an elliptical function of time and distance from the supply ditch.

During furrow irrigation the depth of water intake (Y) at any point (X) along the furrow can be described by a curve such as:

Sketch 1
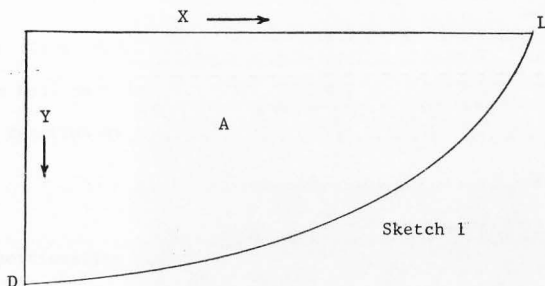
X is the distance in feet down the furrow from the supply ditch, Y is depth in feet of water intake, and A is the area enclosed by the curve and the axis and also the volume (cubic feet) of infiltrated water per foot width of field. If we have a constant inflow rate (Q) at the head of the furrow and neglect the volume of water that remains in the furrow:

$$A = \frac{Q}{W} = \frac{\text{Inflow Rate (Cfm)}}{\text{Furrow spacing (ft)}} \times \text{Time (min)} \qquad (C-1)$$

The term "homogeneous soil" as used here means a soil which has uniform characteristics that do not change with depth or time. Intake rate of such soils has been found to be proportional to the square root of time when gravity forces are negligible. This has been proven on theoretical bases by Washburn (1921). It has been demonstrated in the

laboratory by Biggar and Taylor (1960) and others. And it has been obtained under field conditions by Criddle, Davis, Pair, and Shockley (1956). Mathematically this relation can be expressed:

$$Y = a \ (T-t)^{\frac{1}{2}} \qquad (C-2)$$

where a is the proportionality constant, T is total time of irrigation as in equation (C-1), and t is time required for the surface water to reach the point X in the furrow. T-t is, in other words, the opportunity time at point X.

Since Y is a linear function of the square root of time and A is a function of XY as well as a linear function of time, it follows that X must be a linear function of the square root of time:

$$X = bt^{\frac{1}{2}} \qquad (C-3)$$

b is another proportionality constant. This result is in accord with the data reported by Criddle et al. (1956) for field observations that comply with equation (C-2).

It is proposed that the assumptions and conditions given lead to the proof that the curve in Figure 1 is mathematically a quarter arc of an ellipse. The proof of this consists of using equations (C-2) and (C-3) to show that the focal radii definition of an ellipse also defines the curve in Figure 1.

According to Hart (1957), "an ellipse is the locus of a point for which the sum of the undirected distances to two fixed points is a constant greater than the distance between them."
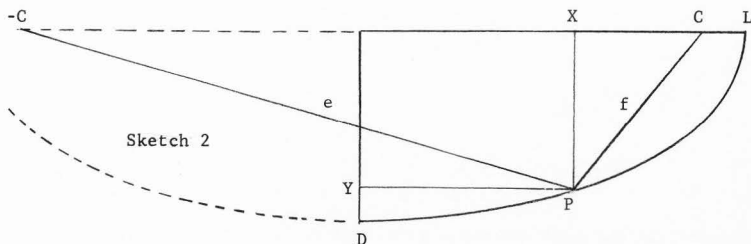
Sketch 2

In Sketch 2, these two undirected distances are labeled e and f.
P is any point (X, Y) on the curve. D is the depth of water intake at
the head of the furrow at the time (T) that water in the furrow has
advanced to point L. C and -C are the foci, defined by the equation

$$C^2 = L^2 - D^2 \qquad (C-4)$$

which is a necessary but insufficient condition to define an ellipse.
The proof that the arc is elliptical rests in showing that the sum of
e and f is a constant for any point P on the curve.

Since $L - bT^{\frac{1}{2}}$ and $D = aT^{\frac{1}{2}}$ then $C^2 = L^2 - D^2 = (bT^{\frac{1}{2}})^2 - (aT^{\frac{1}{2}})^2 = (b^2 - a^2)T$

By Pythagorean Theorem:

$$e^2 = (C + X)^2 + Y^2 = C^2 + 2CX + X^2 + Y^2$$

Substituting for C, X, and Y gives:

$$e^2 = b^2T - a^2T + 2(b^2 - a^2)^{\frac{1}{2}}T^{\frac{1}{2}}(bt^{\frac{1}{2}}) + b^2T + a(T-t)^{\frac{1}{2}}$$

This simplifies to:

$$e^2 = b^2T + 2(b^2 - a^2)^{\frac{1}{2}}T^{\frac{1}{2}}bt^{\frac{1}{2}} + (b^2 - a^2)t \ ,$$

which factors to:

$$e^2 = [bT^{\frac{1}{2}} + (b^2 - a^2)^{\frac{1}{2}}t^{\frac{1}{2}}]^2$$

So $\qquad e = bT^{\frac{1}{2}} + (b^2 - a^2)^{\frac{1}{2}}t^{\frac{1}{2}}$

Similarly for the distance f:

$$f^2 = (C - X)^2 + Y^2 = C^2 - 2CX = X^2 + Y^2$$

Substituting for C, X, and Y gives:

$$f^2 = b^2T - 2(b^2 - a^2)^{\frac{1}{2}}T^{\frac{1}{2}}bt^{\frac{1}{2}} + a(T-t)^{\frac{1}{2}}$$

which simplifies to:

$$f^2 = b^2T - 2(b^2 - a^2)^{\frac{1}{2}}T^{\frac{1}{2}}bt^{\frac{1}{2}} + (b^2 - a^2)t$$

This factors to:

$$f^2 = [bT^{\frac{1}{2}} - (b^2 - a^2)^{\frac{1}{2}}t^{\frac{1}{2}}]^2$$

and $\qquad f = bT^{\frac{1}{2}} - (b^2 - a^2)^{\frac{1}{2}}t^{\frac{1}{2}}$

The sum of e and f is

$$bT^{\frac{1}{2}} + (b^2 - a^2)^{\frac{1}{2}}t^{\frac{1}{2}} + bT^{\frac{1}{2}} - (b^2 - a^2)^{\frac{1}{2}}t^{\frac{1}{2}} = 2BT^{\frac{1}{2}}$$

$BT^{\frac{1}{2}}$ is identical to L, so the sum is always equal to 2L. Therefore the sum of the two distances is constant for any fixed T and does not vary with X and Y, thus the necessary and sufficient conditions are satisfied.

Literature Cited

Biggar, J. W. and Sterling A. Taylor. 1960. Some aspects of the kinetics of moisture flow into unsaturated soils. Soil Sci. Soc. Amer. Proc. 24: 81-85.

Criddle, Wayne D., Sterling Davis, Claude H. Pair, and Dell G. Shockley. 1956. Methods for evaluating irrigation systems. U.S.D.A. Agric. Handbook No. 82. 24 p.

Hart, Wm. L. 1957. Analytic geometry and calculus. D. C. Heath and Co., Boston. p. 49.

Washburn, E. W. 1921. Dynamics of capillary flow. Phys. Rev. 17: 273-283.